Comparative Medicine
Copyright 2019
by the American Association for Laboratory Animal Science

Vol 69, No 5
October 2019
Pages 350–373

Original Research

Influence of Daytime LED Light Exposure on Circadian Regulatory Dynamics of Metabolism and Physiology in Mice

Robert T Dauchy,[1,*] David E Blask,[1] Aaron E Hoffman,[2] Shulin Xiang,[1] John P Hanifin,[4] Benjamin Warfield,[4] George C Brainard,[4] Murali Anbalagan,[1] Lynell M Dupepe,[3] Georgina L Dobek,[3] Victoria P Belancio,[1] Erin M Dauchy,[5] and Steven M Hill[1]

Light is a potent biologic force that profoundly influences circadian, neuroendocrine, and neurobehavioral regulation in animals. Previously we examined the effects of light-phase exposure of rats to white light-emitting diodes (LED), which emit more light in the blue-appearing portion of the visible spectrum (465 to 485 nm) than do broad-spectrum cool white fluorescent (CWF) light, on the nighttime melatonin amplitude and circadian regulation of metabolism and physiology. In the current studies, we tested the hypothesis that exposure to blue-enriched LED light at day (bLAD), compared with CWF, promotes the circadian regulation of neuroendocrine, metabolic, and physiologic parameters that are associated with optimizing homeostatic regulation of health and wellbeing in 3 mouse strains commonly used in biomedical research (C3H [melatonin-producing], C57BL/6, and BALB/c [melatonin-non-producing]). Compared with male and female mice housed for 12 wk under 12:12-h light:dark (LD) cycles in CWF light, C3H mice in bLAD evinced 6-fold higher peak plasma melatonin levels at the middark phase; in addition, high melatonin levels were prolonged 2 to 3 h into the light phase. C57BL/6 and BALB/c strains did not produce nighttime pineal melatonin. Body growth rates; dietary and water intakes; circadian rhythms of arterial blood corticosterone, insulin, leptin, glucose, and lactic acid; pO_2 and pCO_2; fatty acids; and metabolic indicators (cAMP, DNA, tissue DNA ^{3}H-thymidine incorporation, fat content) in major organ systems were significantly lower and activation of major metabolic signaling pathways (mTOR, GSK3β, and SIRT1) in skeletal muscle and liver were higher only in C3H mice in bLAD compared with CWF. These data show that exposure of C3H mice to bLAD compared with CWF has a marked positive effect on the circadian regulation of neuroendocrine, metabolic, and physiologic parameters associated with the promotion of animal health and wellbeing that may influence scientific outcomes. The absence of enhancement in amelatonic strains suggests hyperproduction of nighttime melatonin may be a key component of the physiology.

Abbreviations: bLAD, blue-enriched LED light at day; CWF, cool white fluorescent; dpm, disintegrations per minute; GSK3β, glycogen synthase kinase 3β; ipRGC, intrinsically photosensitive retinal ganglion cell; LED, light-emitting diode; mTOR, mechanistic target of rapamycin; SCN, suprachiasmatic nuclei; SIRT1, nicotinamide adenine dinucleotide-dependent deacetylase sirtuin 1; TFA, total fatty acid

DOI: 10.30802/AALAS-CM-19-000001

Light and lighting protocols in laboratory animal facilities have long been a concern to biomedical researchers and animal care personnel alike. All life varies in its capacity to use visible and nonvisible photic energy. Alternating cycles of light and darkness entrain the master biologic clock, located within the suprachiasmatic nucleus (SCN) in the anterobasal hypothalamus of the brain.[10,50] A small set of cells within the retina of the eyes called the intrinsically sensitive retinal ganglion cells (ipRGC) contain the photopigment melanopsin, which mediates photobiologic responses in circadian rhythms of metabolism and physiology.[1,3,6,18,33,45,48,53,72] Melanopsin ipRGC detect light quanta mostly in the blue-appearing portion of the visible spectrum (465 to 485 nm), and photic information is transmitted to the SCN through the retinohypothalamic tract. The SCN regulates the nighttime pineal gland production of the circadian neurohormone melatonin (N-acetyl-5-methoxytryptamine) that results in high nighttime and low daytime levels.[31] The daily melatonin signal contributes to the temporal coordination of normal behavioral and physiologic functions associated with the promotion of animal health and wellbeing.[3,56] Indeed, as humans age, maintenance of a robust melatonin rhythm, which signifies a strong signal from the SCN, is associated with improved health.[61] Therefore, exposure to light in an intensity-, duration-, and wavelength- (that is, spectrum) dependent manner is essential to regulation of the SCN.[9] Variations in any of these parameters at a given time of day influences endogenous circadian nighttime melatonin levels and may lead to various

Received: 10 Jan 2019. Revision requested: 03 Feb 2019. Accepted: 04 Mar 2019.
Departments of [1]Structural and Cellular Biology, [2]Epidemiology, and [3]Comparative Medicine, Tulane University School of Medicine, New Orleans, Louisiana; [4]Department of Neurology, Thomas Jefferson University, Philadelphia, Pennsylvania; and [5]Department of Medicine, Louisiana State Health Science Center, New Orleans, Louisiana.
[*]Corresponding author. Email: rdauchy@tulane.edu.

age- and disease-related health problems, including metabolic syndrome, obesity, and cancer.[7-9,20,21,28,31,48,56-59]

Recently, we demonstrated that nighttime plasma melatonin levels in rats maintained in daytime light-emitting diode (LED) lighting, enriched in light in the blue-appearing portion of the visible spectrum (bLAD), were 7-fold higher than those in rats maintained in broad-spectrum cool white fluorescent (CWF) lighting.[23,24] Furthermore, the melatonin duration extended 2 to 3 h into the light phase, due to the augmented production of melatonin in the night. In addition, we recently determined that athymic nude mice (Crl:NU(NCr)-*Foxn1*^{nu}), used to support the development of human tumors for our tissue-isolated nude rat model (Crl:NCI-*Foxn1*^{rnu}),[7,8,21,22] are circadian complete (melatonin-producing) and respond in a similar fashion to bLAD as do nude rats (male and female).[23] Most notable was the finding that, in both male and female nude rats and mice exposed to bLAD, compared with daytime full-spectrum CWF light, nighttime melatonin levels were 6- to 7-fold higher, thus significantly inhibiting metabolism, signal transduction activity, and growth of human tumors.[21,22]

In some commonly used strains of mice, however, nighttime pineal melatonin production is impaired or nonexistent.[43] Melatonin is produced in the pineal gland by *N*-acetylation of the precursor serotonin by akylaryl *N*-acetyltransferase (AANAT) followed by *O*-methylation by hydroxyindole-*O*-methyltransferase (HIOMT).[44] Despite some original controversy regarding the C57BL/6 strain,[27,70] it is now generally accepted that the inbred C57BL/6 and BALB/c mouse strains do not produce nighttime pineal melatonin, as both strains are missing active NAT and HIOMT from the pineal gland;[43,69,71] in contrast, the C3H strain expresses both enzymes and displays a robust nighttime pineal melatonin surge.[43,69] C57BL/6 mice have a point mutation in the AANAT gene, resulting in a truncated protein with little-to-no enzyme activity.[59] One of the aims of our current study was to determine whether, in the absence of the normal nighttime melatonin signal, bLAD lighting may nonetheless influence circadian rhythms of metabolism and physiology in the C57BL/6 and BALB/c strains and, ultimately, animal health and wellbeing.

Institutions around the world are rapidly transitioning to the emerging LED technology due primarily to improved efficiency, lower heat production, markedly longer operating life, and overall cost savings.[23,26,35,40,54] The American Medical Association has released 2 public health reports on the effects of nighttime LED lighting on humans and the environment.[16,17] The reports reviewed current research on the biologic and behavioral effects of light. The most recent report covers primarily nighttime LED outdoor street lighting in the community as it pertained to visibility glare, visual impairment due to stray light, and the putative environmentally disruptive effects of high-intensity LED light (including blue spectrum light) on humans and nocturnal animals.[16] The 2016 American Medical Association report elicited some response and controversy from the lighting and energy communities.[41,68]

The 8th edition of the *Guide for the Care and Use of Laboratory Animals*,[39] as well as several prior editions, focuses primarily on retinopathy concerns in rodents relative to vivarium lighting. Little to no mention is made regarding circadian regulation by light and lighting protocols in the brief section devoted to animal facility lighting. In addition, little information is available concerning the potential influence of different types of lighting such as LED lighting on animal health and wellbeing. Furthermore, scientific consensus on the methods for quantifying and reporting light stimuli in experimental studies has occurred only recently.[48] Following these recommended practices will facilitate comparing results across investigations. This consensus was adapted into a balloted report and distributed internationally.[14] More recently this consensus has been developed into an international standard.[15] Therefore, our laboratory aims to report as thoroughly as possible all light measurements necessary for replication of experimental conditions, enabling comparison of results across investigations, including comprehensive spectral power distribution measurements, which are currently the most appropriate and accepted methodology available in the lighting industry.[11,14,15,48]

Increasingly, our 24/7 global society is exposed to primarily broad-spectrum light at night (LAN) and bLAD in the workplace and home environment—one of the most profound environmental changes to occur since the advent of the electric light bulb 130 y ago.[16,40] Prior to this invention and the onset of the industrial revolution, our global societies were exposed primarily to blue-enriched environmental light during daytime and, if any light at night, long-spectrum (yellow to red) nighttime light (oil lamps, candles, wood fires) through thousands of years of evolution.[54] Even before animal life evolved on our planet there existed a night–day (blue-enriched light) cycle.[10,48,54] It is understandable, then, how the light:dark cycle has had an impact on our development and evolution over the millennia. Evidence strongly suggests that the use of the more natural daytime blue-enriched LED light in animal facilities, compared with broad-spectrum incandescent and CWF light, has a marked positive effect on the circadian regulation of behavioral, neuroendocrine, metabolic, and physiologic parameters associated with the promotion of animal health and wellbeing and thereby influences scientific outcomes.[23] In our previous studies,[23,24] using a new light metric[48] to assess our findings, we provided compelling evidence that animals exposed to bLAD compared with CWF lighting displayed characteristics of enhanced health and wellbeing.

With these concerns in mind, the overall goal of this study was to examine the influence of bLAD light, as compared with broad-spectrum CWF light, on metabolic and physiologic measures of laboratory animal health and wellbeing. Specifically, we examined the hypothesis that the spectral characteristics (wavelength) of bright LED light during the light phase, compared with standard CWF lighting, not only amplifies the normal circadian nocturnal melatonin signal but also alters the circadian regulation of plasma measures of metabolism and physiology in these important strains of mice to the fields of laboratory animal science and biomedical research.

Materials and Methods

Animals, housing conditions, and diet. Male and female inbred mice (C3H [Charles River Lab strain code 025; n = 60 male; n = 60 female]; C57BL/6 [CRL strain code 027; n = 60 male; n = 60 female]; and, BALB/c inbred [CRL strain code 028 n = 60 male; n = 60 female]; age, 3 to 4 wk of age) used in this study were purchased from Charles River (Wilmington, MA). Animals were maintained in an AAALAC-accredited facility in accordance with the *Guide for the Care and Use of Laboratory Animals*.[39] All procedures for animal use were approved by the Tulane University IACUC. In addition, this study adheres to NIH principles and guidelines regarding strict application of the scientific method to ensure robust and unbiased experimental design, methodologies, analysis, rigor and reproducibility, and transparency in reporting.[13]

Mice were maintained as described following in autoclaved cages containing hardwood maple bedding (no. 7090, Sanichips,

Harlan Teklad, Madison, WI; 3 bedding changes weekly). To ensure that all animals remained infection-free from both bacterial and viral agents, serum samples from sentinel animals were tested quarterly and during the course of this study by using Multiplex Fluorescent Immunoassay 2 (IDEXX Research Animal Diagnostic Laboratory, Columbia, MO), as described previously.[19-23] All mice were free of the following pathogens: mouse hepatitis virus, minute virus of mice, mouse parvovirus, mouse norovirus, Theiler murine encephalomyelitis virus, mouse rotavirus, Sendai virus, pneumonia virus of mice, reovirus 3, lymphocytic choriomeningitis virus, ectromelia virus, mouse adenovirus types 1 and 2, mouse polyoma virus, mouse cytomegalovirus, *Encephalitozoon cuniculi,* cilia-associated respiratory bacillus, *Clostridium piliforme*, and *Mycoplasma pulmonis.* In addition, mice were negative for Heliobacter spp. (real-time PCR analysis of feces) and free of endo- and ectoparasites. Throughout this study, animals were assessed daily for food and water intake and body weight changes. Food spillage and water evaporation has been reported to be less than 0.1 g per mouse daily and 0.2 mL per 48 h, respectively, for these strains of mice and were therefore not taken into account here.[4] Eight independent determinations of this diet revealed that it contained 4.72 g total fatty acid (TFA) per 100 g of diet composed of 0.78% myristic (C14:0), 13.68% palmitic (C16:0), 1.05% palmitoleic (C16:1n7), 3.62% stearic (C18:0), 20.58% oleic (C18:1n9), 52.10% linoleic (C18:2n6), 7.82% γ-linolenic, and 0.18% arachidonic (C20:4n6) acids. Minor amounts of other FA comprised 0.19%. Conjugated linoleic acids (CLAs) and *trans* FAs were not found. More than 90% of the TFA was in the form of triglycerides; more than 5% was in the form of free fatty acids.

Caging, lighting, and spectral transmittance measurements. After a 1-wk acclimation period, mice were randomized, taking into account strain and sex, into 2 designated groups of control (standard cool white fluorescent lighting; CWF) and experimental (blue-enriched LED lighting at daytime, bLAD) in standard translucent laboratory mouse cages; the study timeline was 12 wk. Standard mouse cages (polycarbonate translucent clear, catalog no. N10; 7.5 in. × 11.5 in. × 5 in.; wall thickness, 0.10 in.), wire bar lids (catalog no. N10SS), and microfilter tops (catalog no. N10NBT) used in this study were purchased from Ancare (Bellmore, NY). The SPF mice were maintained in environmentally controlled rooms (25 °C; 50% to 55% humidity) with 12:12-h diurnal lighting (lights on, 0600). The CWF control animal room was lighted with a series of 2 overhead luminaires containing 4 standard soft, cool-white (2700 lm; 4100 correlated color temperature) fluorescent lamps per ballast (F32T8TL841, model 272484, Alto II Collection T8 [diameter, 1 in.; tubular] 32 W, 48 in., series 800, Philips, Somerset, NJ). The experimental LED animal room was lighted with a series of 2 overhead luminaires containing 4 Philips LED lamps, high in emission of blue-appearing portion of the visible spectrum (465 to 485 nm; 2650 lm, >5000 correlated color temperature) lamps per ballast (model 9290011242, 12T8/AMB/48, T8, 12 W, 48 in., Philips). Photo images, along with radiometric and photometric values, of the study lamps were reported previously.[22-24] Animal rooms were completely devoid of light contamination during the dark phase.[7,8,19-24]

Daily during the course of this experiment, the animal room was monitored for normal light-phase lighting intensity at 1 m above the floor in the center of the room (at rodent eye level) and outside, from within, and at the front of the animal cages. Irradiance measures were recorded by using a radiometer–photometer (IL-1400A, International Light Technologies, Peabody, MA) with a silicon diode detector head (catalog no. SEL033) with a wide-angle input optic (catalog no. W6849) and a filter (catalog no. F23104) that provided a flat response across the visible spectrum. Illuminance measures used a silicon diode detector head (catalog no. SEL033) with a wide-angle input optic (catalog no. W10069) and a filter (catalog no. Y23104) to provide a photopic illuminance response. The meter and associated optics were calibrated annually, as described previously.[19-23] Each day and at the same time (0800), prior to light intensity measurements for that day, all cages on the static rack shelf were rotated one position to the right (placed at an identical, premeasured distance apart) in the same horizontal plane; the cage at position 6 (last position at far right on the shelf) was moved to position 1 (first position at far left on the shelf) on the next lower shelf. Although there were no significant differences in light intensity, as measured outside and from within the front of each cage at each of the 36 positions, the daily cage shift further ensured uniformity of intensity of ocular light exposure and accounted for the effects of any unforeseen subtle differences due to the position on the rack shelf.

Under current convention, when discussing human and laboratory animal environments, the term lux is employed, indicating the amount of light falling on a surface that stimulates the mammalian eye during the daytime, that is, the perceived brightness to the eye (photometric values). Measures of lux are appropriate for human daytime vision but are not appropriate for quantifying light stimuli that regulates circadian, neuroendocrine or neurobehavioral physiology in animals or humans.[10,31,48] Consequently, radiometric values of irradiance ($\mu W/cm^2$) were measured in the cages by using the radiometric detector described earlier. Irradiance quantifies the radiant power of light over a defined bandwidth of electromagnetic energy.[48] Given these standards, the light stimuli in the investigation reported here are presented in terms of both lux and $\mu W/cm^2$ for ease of understanding.

Spectral power measurements. The lamps were installed in an overhead T8 assembly in a lightproof room, and then the spectral characteristics of each light source were measured separately by using a handheld spectroradiometer (ASD FieldSpec, ASD, Boulder, CO) with a cosine receptor attachment, as described previously.[19,21-23]

Calculation of effective rod, cone, and melanopsin photoreceptor illuminances. To calculate the effective rodent rod, cone, and melanopsin photoreceptor illuminances, the light sources were entered into a Toolbox worksheet, which is a software model for rodent photoreception freely available online.[52] The spectral power distributions for the experiments shown here were imported into the worksheet in 1-nm increments between 325 and 782 nm. The Toolbox lists the rodent spectral range as extending to 298 nm, outside the range of the spectroradiometer used in this study. According to Toolbox instructions, values between 298 and 325 nm were manually changed to 0.

Tissue collection. After a total of 12 wk (84 d) under the lighting regimens described earlier, animals were prepared for tissue collection (whole blood, liver, left retroperitoneal fat pad, left quadriceps femoris skeletal muscle, heart, lungs, kidneys, duodenum, brain, testes, ovaries) over the next 36-h period at 6 circadian times (1200, 1600, 2000, 2400, 0400, and 0800) during an 12:12-h light:dark cycle. All procedures were conducted using asceptic techniques. Briefly, mice were anesthetized with ketamine (80 mg/kg) and xylazine (9.80 mg/kg) intraperitoneally by using a 1-mL, 25-gauge tuberculin syringe (Becton Dickenson; Franklin Lakes, NJ). After the appropriate plane of anesthesia (lowered respiration rate; pedal reflex test) was achieved, the mouse was then placed on a heating pad in the

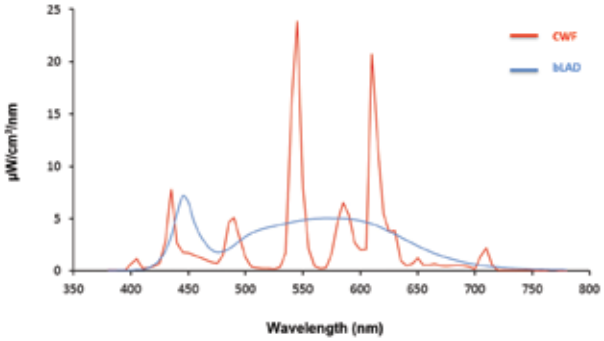

Figure 1. Normalized spectral power distributions of the polychromatic blue-enriched LED (blue) and fluorescent lamp (red) light as transmitted through a standard polycarbonate, translucent laboratory mouse cage.

surgical area, with the head facing the surgeon. The neck area was shaved and cleaned to remove hair, and a small incision (1 cm) was made to expose the right jugular vein and carotid artery. A small amount of [^{3}H]thymidine (0.05 µCi in 20 µL sterile saline) was injected into the jugular vein and allowed to circulate for a period of 1 min. Next, the carotid artery was ligated, and arterial whole blood was allowed to flow freely into a collection minivial as the mouse was exsanguinated. A portion of the arterial blood collected was immediately measured for glucose, lactate, pO_2, pCO_2, pH, Hct, and Hgb by using an VetScan iSTAT1 Analyzer and iSTAT1 G4$^+$ (no. 600-9000-25) and G8$^+$ (no. 600-9001-25) cartridges (Abaxis, Union City, CA). Values for glucose and lactate are reported as mg/dL and mmol/L, and for pO_2 and pCO_2 as mm Hg, respectively. Minimal detection levels for pH, pO_2, pCO_2, glucose, and lactate values were 0.01, 0.1 mm Hg, 0.1 mm Hg, 0.2 mg/dL and 0.01 mmol/L, respectively.

Finally, all remaining tissues were rapidly removed from the euthanized mouse and snap-frozen under liquid nitrogen for future analysis. During dark phase, this process is completed under low-intensity (less than 35 lx) red safety light, as previously described.[7,8,19-23] The entire procedure required approximately 5 min per mouse. Remaining arterial whole blood samples were centrifuged and serum samples frozen (–20 °C) for future analysis.

Melatonin analysis. Arterial plasma melatonin levels were measured by using a melatonin ^{125}I radioimmunoassay kit (catalog no. 01-RK-MEL2, Alpco, Salem, NH; lot no. 1429.18, prepared by Bühlmann Laboratories, Schönenbuch, Switzerland) and analyzed by using a Cobra 5005 Automated Gamma Counter (Packard, Palo Alto, CA), as previously described.[7,8,19-23] The minimal detection level for the assay was 1 to 2 pg/mL plasma.

FA extraction and analysis. Arterial plasma TFA, as well as tissue TFA, were extracted from 0.1 mL arterial and venous samples after the addition of heptadecanoic acid (C17:0), methylated, and analyzed through gas chromatography as previously described.[7,8,19-20] Values for TFA represent the sum of the 7 major fatty acids (myristic, palmitic, palmitoleic, stearic, oleic, linoleic, and arachidonic acids) in the blood plasma. Tissue TFA in control and experimental groups were extracted from 0.2 mL of 20% homogenates, as previously described.[7,8,19-23] The minimal detectable limit for the assay was 0.05 µg/mL.

ELISA analysis of corticosterone, insulin, and leptin. Arterial plasma samples were prepared in duplicate for measurement of corticosterone (catalog no. 55-CORMS-E01, mouse/rat, protocol version 09/06/17, Alpco), insulin (catalog no. 80-INSMSH-E01, E10, mouse, high range, protocol version 09/14/17, Alpco), and leptin (catalog no. 22-LEPMS-E01, mouse/rat, protocol version

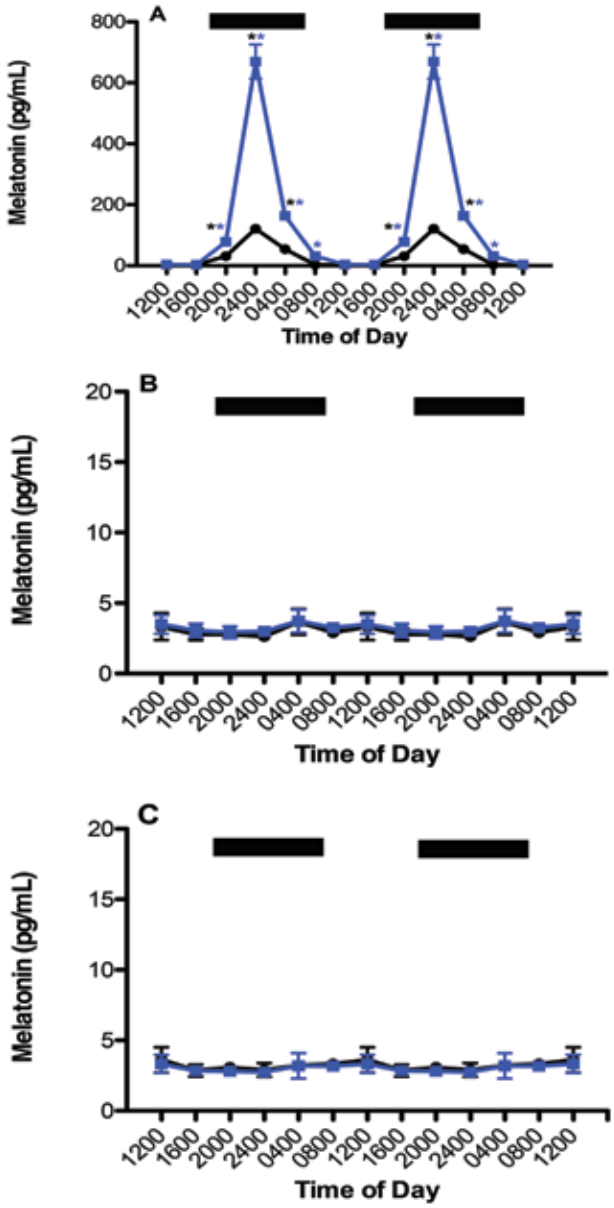

Figure 2. Circadian plasma melatonin levels (mean ± 1 SD) of male and female pigmented (A) C3H and (B) C57BL/6 and nonpigmented BALB/c (C) mice maintained for 12 wk in standard, polycarbonate, translucent, clear cages under CWF (controls, solid black circles) or bLAD (experimental, solid blue squares) lighting with a 12:12-h light:dark phase (300 lx; 123 µW/cm^2). During the 12-h dark phase lighting conditions from 1800 to 0600 (dark bars), animals were exposed to no light at night. Data are plotted twice in panels to better demonstrate rhythmicity and clarity of scale. Rhythmicity analysis (Table 3) revealed robust and highly significant ($P < 0.0001$) rhythmic patterns under control lighting conditions for both groups of C3H mice but not for C57BL/6 and BALB/c mice, with 31.9-fold and 230.9-fold increases in nighttime amplitudes compared with daytime in CWF and bLAD in C3H mice, respectively, and a 5.2-fold increase in amplitude observed in bLAD-exposed C3H mice compared with controls at 2400 ($P < 0.001$; Student t test). Concentrations with asterisks (black, CWF peaks; blue, bLAD peaks) differ ($P < 0.05$) from concentrations without asterisks.

030112, Alpco) by using chemiluminescent ELISA diagnostic kits. Samples were measured by using a VersaMax microplate reader

Table 1. Calculated radiometric values, photopic illuminances v(λ), and mouse photopigment illuminances (α-opic lux) of the polychromatic LED and fluorescent light sources as transmitted through the cage[48,55]

	Radiometric and photometric values (325–780 nm inclusive)			Rodent retinal photopigment weighted illuminances (α-opic lux)			
	Photon flux (cm^2/s)	Irradiance ($\mu W/cm^2$)	Photopic illuminance (lux)	S cone	Melanopsin ipRGC	Rod	M cone
Cage transmittance, bLAD	5.62E+14	203	646	29	437	478	502
Cage transmittance, CWF	5.10E+14	182	657	20	305	373	416

Table 2. Effects of CWF and bLAD lighting on food intake (g /100 g body weight daily), water intake (mL/100 g body weight daily), and animal growth rates (g/d) in C3H, C57BL/6, and BALB/c male and female mice during maintenance phase

	C3H				C57BL/6				BALB/c			
	CWF		bLAD		CWF		bLAD		CWF		bLAD	
	M	F	M	F	M	F	M	F	M	F	M	F
Food	19.88 ± 0.17	20.93 ± 0.13[a]	18.56 ± 0.09[a,b]	19.55 ± 0.06[a-c]	21.09 ± 0.23[a,c,d]	22.02 ± 0.22[a-e]	21.44 ± 0.18[a-d,f]	22.18 ± 0.26[a-g]	19.26 ± 0.12[a-h]	22.46 ± 0.16[a-g]	19.66 ± 0.19[b-h]	22.10 ± 0.17[a-e,g,i,k]
Water	19.11 ± 0.06	19.13 ± 0.10	19.62 ± 0.07[a,b]	19.87 ± 0.11[a-c]	18.49 ± 0.25[a-d]	20.82 ± 0.29[a-e]	16.22 ± 0.24[a-f]	19.46 ± 0.30[a-g]	16.67 ± 0.19[a-h]	18.64 ± 0.13[a-e,g]	16.93 ± 0.13[b-f]	19.08 ± 0.17[c-g,i-k]
Growth	0.220 ± 0.035	0.150 ± 0.0180[a]	0.111 ± 0.001[a,b]	0.071 ± 0.001[a-c]	0.146 ± 0.020[a,c,d]	0.113 ± 0.021[a,b,d,e]	0.147 ± 0.014[a,c,d,f]	0.099 ± 0.010[a-g]	0.120 ± 0.020[a-e,g,h]	0.074 ± 0.017[a-i]	0.113 ± 0.021[a-e,h-j]	0.070 ± 0.011[a-i,k]

F, female; M, male
Values represent means ± 1 SD (n = 30/group; that is, 30 males and 30 females in each lighting environment per strain)
[a]$P < 0.05$ compared with value for C3H mice in male CWF control group.
[b]$P < 0.05$ compared with value for C3H mice in female CWF control group.
[c]$P < 0.05$ compared with value for C3H mice in male bLAD experimental group.
[d]$P < 0.05$ compared with value for C3H mice in female bLAD experimental group.
[e]$P < 0.05$ compared with value for C57BL/6 mice in male CWF control group.
[f]$P < 0.05$ compared with value for C57BL/6 mice in female bLAD experimental group
[g]$P < 0.05$ compared with value for BALB/c mice in male CWF control group.
[h]$P < 0.05$ compared with value for BALB/c mice in male experimental control group.

(Molecular Devices, Sunnyvale, CA) at 450 nM. Detection sensitivities for corticosterone, insulin, and leptin plasma analyses were respectively 6.1 ng/mL, 0.52 ng/mL, and 10 pg/mL, and the coefficient of variation for all assays was less than 8.0%.

Determination of [^{3}H]thymidine incorporation into tissue DNA, DNA content, and tissue cAMP content. [^{3}H]thymidine incorporation into tissue DNA, DNA content, and metabolic tissue levels of cAMP (ELISA, GE Lifesciences, Piscataway, NJ) were determined as described previously.[7,8,19-23]

Western blot measurement of tissue phosphorylated kinases. Excised animal organs were extracted and analyzed for signal transduction activity (that is, Akt/mTOR, GSK3β, and SIRT1), as previously described.[7,8,19-23]

Statistical analysis. Unless otherwise noted, all data are presented as the mean ± 1 SD (Figure 2 through 10: n = 5 male and n = 5 female mice per time point per strain; Tables 1 through 8: n = 30 male and 30 female mice for each strain in each CWF and bLAD experimental group; n = 360 mice total). The nonparametric JTK_CYCLE algorithm,[36] as implemented in scripts for the R software package (R version 3.1.0; http//openwetware.org/wiki/HughesLab:JTK Cycle), was used to determine the statistical significance of 24-h cycling for each analyte, with adjustments for multiple comparison. This algorithm also was used to determine phase (time of peaks) and amplitude of cycling. Statistical differences between mean values in group bLAD compared with the control CWF group at each circadian time point were assessed by using an unpaired Student test. A P value of less than 0.05 was considered to indicate a significant difference compared with the baseline values within each group. Statistical differences among group means were determined by using one-way ANOVA followed by the Bonferroni multiple comparison test. Student tests and one-way ANOVA followed by Bonferroni posthoc testing were all performed by using Prism 5 (GraphPad Software, La Jolla, CA).

Results

Animal-room illumination and spectral comparisons. Animal room illumination during light phase at the center each room and at 1 m above the floor (with the detector facing upward toward the luminaires) varied minimally (n = 240 measurements). Illuminance and irradiance values were 500.78 ± 2.65 lx (204.40 ± 1.08 $\mu W/cm^2$) in the control CWF room and 494.76 ± 7.11 lx (201.1 ± 2.89 $\mu W/cm^2$) in the experimental bLAD room. Measurements of photometric illuminance (lux) and radiometric irradiance ($\mu W/cm^2$) within the cages of each group are a result of a mean of the values taken at 6 locations within the cages with the detector facing forward (front, center, and rear on right and left sides of cage) at all cage positions to accurately account for actual ocular light levels within the cages independent of the animal location. Average interior ocular light levels showed little to no intercage or intergroup variability (n = 216 measurements per cage per rack) and are reported here for the CWF and bLAD groups, respectively, as 72.50 ± 3.52 lx (29.59 ± 1.44 $\mu W/cm^2$) and 65.14 ± 6.91 lx (26.05 ± 2.76 $\mu W/cm^2$). Normalized spectral power distributions of the T8 lights used in this study, as transmitted through the cage, are shown in Figure 1. The fluorescent lamp shows signature peaks in the appropriate wavelengths (545 and 612 nm) for this type of light. The LED lamp shows a standard blue LED phosphor spectral power distribution with a peak at 448 nm. In terms of total energy in the 465- to 485-nm range, the LED lamp had 65% higher emissions than the CWF lamp. Table 1 provides the calculated photon flux, irradiances, and weighted rodent photopigment illuminances

Table 3. Summary of JTK_CYCLE analysis for mice maintained in control CWF and experimental bLAD lighting environments

	Estimated Peak Phase[a]		Phase Shift[b] (hrs)	Amplitude[a]		Fold Change[b]	Q-value for Circadian Cycling[a]	
	CWF	bLAD		CWF	bLAD		CWF	bLAD
C3H mice								
Corticosterone	18:00	18:00	0	3.72E-05	2.27E-05	1.64	NS	2.85E-02
Glucose	14:00	14:00	0	5.41	4.90E-05	1.10E+05	4.55E-05	8.29E-11
Insulin	2:00	4:00	+2	1.94	2.20	−1.13	7.11E-08	1.46E-04
Lactate	12:00	18:00	+6	0.00	5.80E-02	—	1.29E-03	3.05E-04
Leptin	22:00	24:00	+2	0.67	0.51	1.32	7.11E-08	2.30E-10
Melatonin	02:00	02:00	0	36.94	113.06	−3.06	8.29E-11	2.60E-14
pCO_2	NE[d]	22:00	—	NE[e]	0.64	—	8.20E-04	NS
pO_2	14:00	14:00	0	7.78	3.89	2.00	2.97E-10	1.86E-06
TFA	04:00	04:00	0	1328.09	982.88	1.35	2.43E-22	2.43E-22
C57BL/6 mice								
Corticosterone	1800	NE[d]	—	2.18E–05	NE[e]	—	4.42E–02	2.42E–01
Glucose	1400	1400	0	5.05	5.24	−1.04	2.77E–05	5.22E–05
Insulin	0200	0200	0	1.91	1.90	1.00	2.22E–09	1.32E–09
Lactate	1400	1400	0	0.04	0.03	1.17	7.40E–03	1.49E–02
Leptin	2200	2200	0	0.70	0.70	1.00	7.11E–08	7.11E–08
Melatonin	NE[d]	1000	—	NE[e]	0.16	—	NS	NS
pCO_2	1400	1400	0	9.86E–06	0.16	−1.66E+04	3.95E–03	5.97E–03
pO_2	1400	1400	0	8.49	7.78	1.09	1.41E–12	1.09E–13
TFA	0400	0400	0	719.97	700.74	1.03	1.33E–20	4.73E–21
BALB/c mice								
Corticosterone	NE[d]	1800	—	NE[e]	3.23E–05	—	NS	1.91E–02
Glucose	1400	1400	0	5.47	5.87	−1.07	4.55E–05	3.78E–05
Insulin	0200	0200	0	1.88	1.87	1.01	7.04E–10	9.00E–10
Lactate	NE[d]	1400	—	NE[d]	0.03	—	1.44E–02	5.24E–03
Leptin	0200	0200	0	0.60	0.66	−1.11	2.07E–11	6.13E–12
Melatonin	1000	0200	+8	0.34	37.32	−109.47	NS	6.82E–13
pCO_2	1400	1400	0	5.00E–15	0.07	−1.42E+13	5.97E–03	2.29E–03
pO_2	1400	1400	0	7.78	8.49	−1.09	2.06E–10	2.99E–14
TFA	0400	0400	0	1156.38	1074.34	1.08	2.43E–22	2.92E–17

NS, not significant

[a]Phase-, amplitude-, and multiple-testing-adjusted *P* value (Q) estimated by using JTK_CYCLE analysis with a fixed 24-h period and original units described in the text.

[b]Phase difference and fold change are for the bLAD group relative to the the CWF group. A decrease in bLAD amplitude with regard to CWF is a negative value; an increase is represented by a positive value.

[c]NE, not estimated (JTK_CYCLE analysis did not converge on a single peak phase or amplitude; a value was not provided)

for both lights used, as transmitted through the cage. The data illustrate that, although photon flux and irradiance are relatively similar in the 2 lights, there are marked differences in stimulation of the rodent photoreceptors. In terms of the potential light stimulation to the melanopsin-containing ipRGC, the LED lamp had more than 43% higher emissions than the CWF lamp. In addition, compared with the CWF lamp, the LED lamp had 45%, 28%, and 21% higher emissions for potential light stimulation of the S cones, rods, and M cones, respectively.

Animal food and water intakes and body growth measurements. Food and water intakes and body growth rates differed significantly ($P < 0.05$) between the male and female mice in all strains during the course of the study (Table 2). These parameters differed significantly ($P < 0.05$) in C3H male and female mice maintained in the CWF compared with the bLAD lighting regimen but not in C57BL/6 or BALB/c mice ($n = 90$ measurements/group). On the basis of grams of intake per 100 g body weight[22] in either CWF or bLAD lighting environments, female mice consumed approximately 4.6% ± 0.9% more food daily in both C3H and C57BL/6 strains and 14.8% ± 2.2% more food daily in the BALB/c strain. There were no within-sex differences in food consumption in the C57BL/6 and BALB/c strains maintained in either the CWF or bLAD lighting environments. However, for the C3H mouse strain, male and female mice in the CWF group consumed 7.1% ± 0.1% and 7.2% ± 0.9% more food daily, as compared with bLAD groups. In terms of milliliters per 100 g of body weight daily water consumption,[2] in either CWF or bLAD lighting environments, female mice consumed 0.7% ± 0.1% more water daily in the C3H strain and 14.3% ± 3.8% more water daily in the C57BL/6 and BALB/c strains, compared with male mice ($n = 90$ measurements/group). Within-sex daily water consumption was significantly ($P < 0.05$) greater in C57BL/6 (males, 14.0% ± 0.1%; females, 7.0% ± 0.1%) mice maintained in CWF compared with bLAD lighting environments and lower in both C3H (males, 2.4% ± 0.1%; females, 3.9% ± 0.2%) and BALB/c (males, 1.6% ± 0.3%; females, 2.4% ± 0.3%) mice.

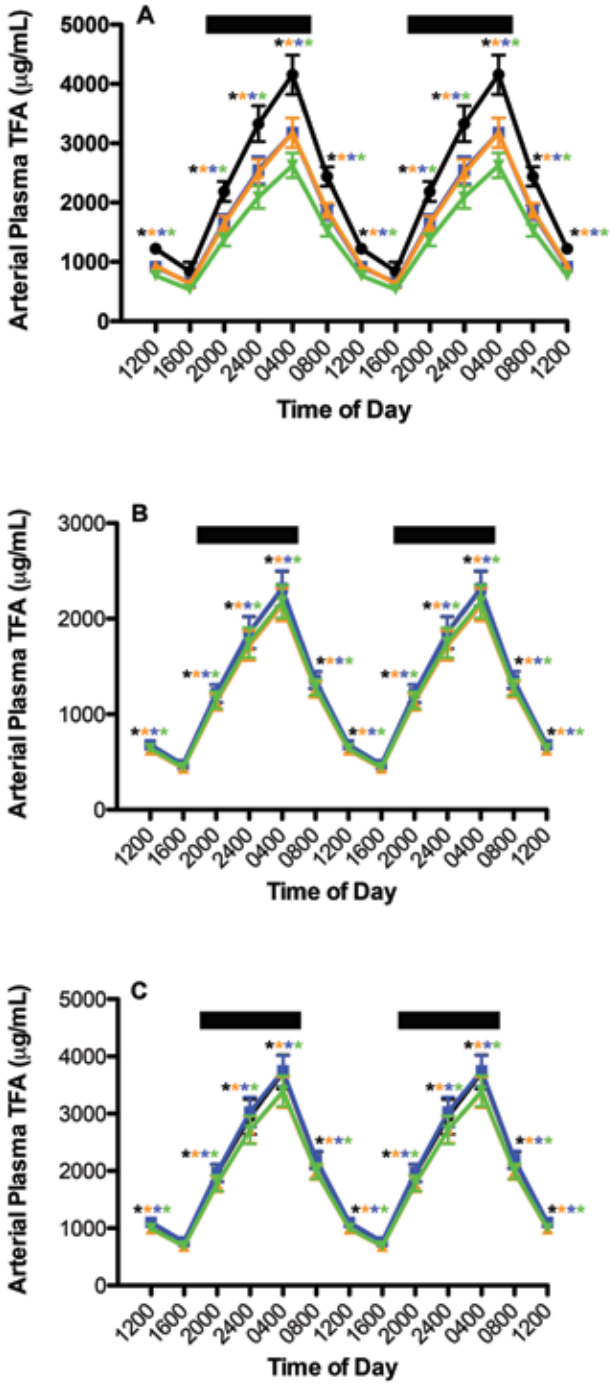

Figure 3. Circadian changes in the blood plasma total fatty (TFA) levels (µg/mL; mean ± 1 SD) of male and female (A) C3H, (B) C57BL/6, and (C) BALB/c mice fed normal chow without restriction and maintained under either control CWF (TFA, male, solid black circles; female solid amber triangles) or experimental bLAD (TFA, male, solid blue squares; female, inverted green triangles) lighting conditions. Mice were exposed to dark-phase lighting conditions (see Methods) from 1800 to 0600 (dark bars). TFA values (mean ± 1 SD; $n = 60$ per group) are the sums of myristic, palmitic, palmitoleic, stearic, oleic, linoleic, and arachidonic acid concentrations collected at the various time points. Data are plotted twice to better demonstrate rhythmicity. Rhythmicity analysis (Table 3) revealed robust and highly significant ($P < 0.0001$) rhythmic patterns under control lighting conditions for both groups, with a more than a 6-fold increase in nighttime amplitude in CWF control and bLAD experimental groups. Concentrations indicated by asterisks are different ($P < 0.05$) from those without asterisks.

Animal growth rates (grams daily) revealed marked differences in both sexes (males gained more than females) of animals maintained in bLAD compared with CWF lighting environments in the C3H strain but not the C57BL/6 or BALB/c strains. Male and female C3H mice grew at a rate of 49.6% ± 0.8% and 52.7 ± 0.5% more slowly in bLAD compared with CWF lighting ($P < 0.05$), respectively, during the maintenance phase. Final body weights at time of the tissue harvest were 26.3 ± 1.8 g for males and 23.3 ± 1.2 g for females in the C3H strain, 28.9 ± 1.4 g for males and 25.0 ± 1.5 g for females in the C57BL/6 strain, and 29.3 ± 1.5 g for males and 22.3 ± 2.2 g for females in the BALB/c strain for control CWF groups, as compared with 23.3 ± 1.2 g for males and 19.9 ± 1.2 g for females in the C3H strain, 29.9 ± 1.2 g for males and 24.0 ± 0.7 g for females in the C57BL/6 strain; and 29.0 ± 1.0 g for males and 21.8 ± 0.9 g for females in the BALB/c strain for experimental bLAD groups.

Plasma melatonin levels. Circadian rhythms in concentrations of plasma melatonin for the 3 mouse strains in CWF and LED lighting are shown in Figure 2. In each strain, plasma melatonin levels did not differ significantly between male and female mice, so values were combined. The overall patterns of daily plasma melatonin level rhythms was similar for both CWF and bLAD groups in the respective strains of mice: low during daytime (less than 4 pg/mL) and significantly ($P < 0.001$) higher during the dark phase, with peak levels occurring between 2400 and 0400 and decreasing to a nadir between 1200 and 1600 in C3H mice and consistently low in both the C57BL/6 and BALB/c strains throughout the 24-h day (Table 3). Significant differences in either the peak height and phase duration of the nocturnal melatonin signal between the CWF and bLAD groups were present only in the C3H mice. In the C3H strain, melatonin levels in the bLAD group began to rise rapidly after the onset of the dark phase, reaching nearly 70% of the peak of those in the CWF group (control) by 2000. However, the peak dark-phase melatonin level for C3H mice in the bLAD group (that is, at 2400) was nearly 6-fold higher ($P < 0.0001$) than that in control mice at the same time point. Arterial plasma melatonin levels remained more than 11-fold higher ($P < 0.05$) in bLAD compared with CWF, even at 2 to 3 h after the onset of light phase, and did not reach normal daytime levels (less than 10 pg/mL) until 1200. The integrated mean levels of melatonin over the 24-h period for bLAD mice (951.1 pg/mL) were more than 4-fold higher than those of animals in CWF (216.4 pg/mL; $P < 0.001$).

Plasma measures of TFA. Circadian rhythms in the concentrations of arterial blood plasma TFA were measured in mice with free access to the food (Figure 3). As a rule, the integrative mean of plasma TFA for each strain over a 24-h day (mg/mL) was C3H > BALB/c > C57BL/6. The plasma pattern of lipid levels in the experimental bLAD mice followed that of the control animals in all strains, similar to that reported earlier in rats.[19,21,22] Daily levels in TFA between male and female mice were significantly ($P < 0.001$)different in all 3 strains (Figure 3 A through C) in both CWF and bLAD groups. Total TFA areas assessed over the 24-h day for the C3H within-sex curves (Figure 3 A) were 14.17 ± 0.20 mg/mL for males and 10.79 ± 0.14 mg/mL for females in CWF groups and 10.76 ± 0.14 mg/mL for males and 8.39 ± 0.12 mg/mL for females in bLAD groups. Total TFA areas assessed over the 24-h day for the C57BL/6 (Figure 3 B) and BALB/c (Figure 3 C) mouse curves shown for CWF compared with bLAD revealed no within-sex differences and were, respectively, 7.89 ± 0.10 mg/mL for males and 7.92 ± 0.10 mg/mL for females compared with 7.32 ± 0.10 mg/mL for males and 7.44 ± 0.10 mg/mL for females in the C57BL/6 strain, respectively, and 12.68 ± 0.20 mg/mL for males and 12.81 ± 0.20

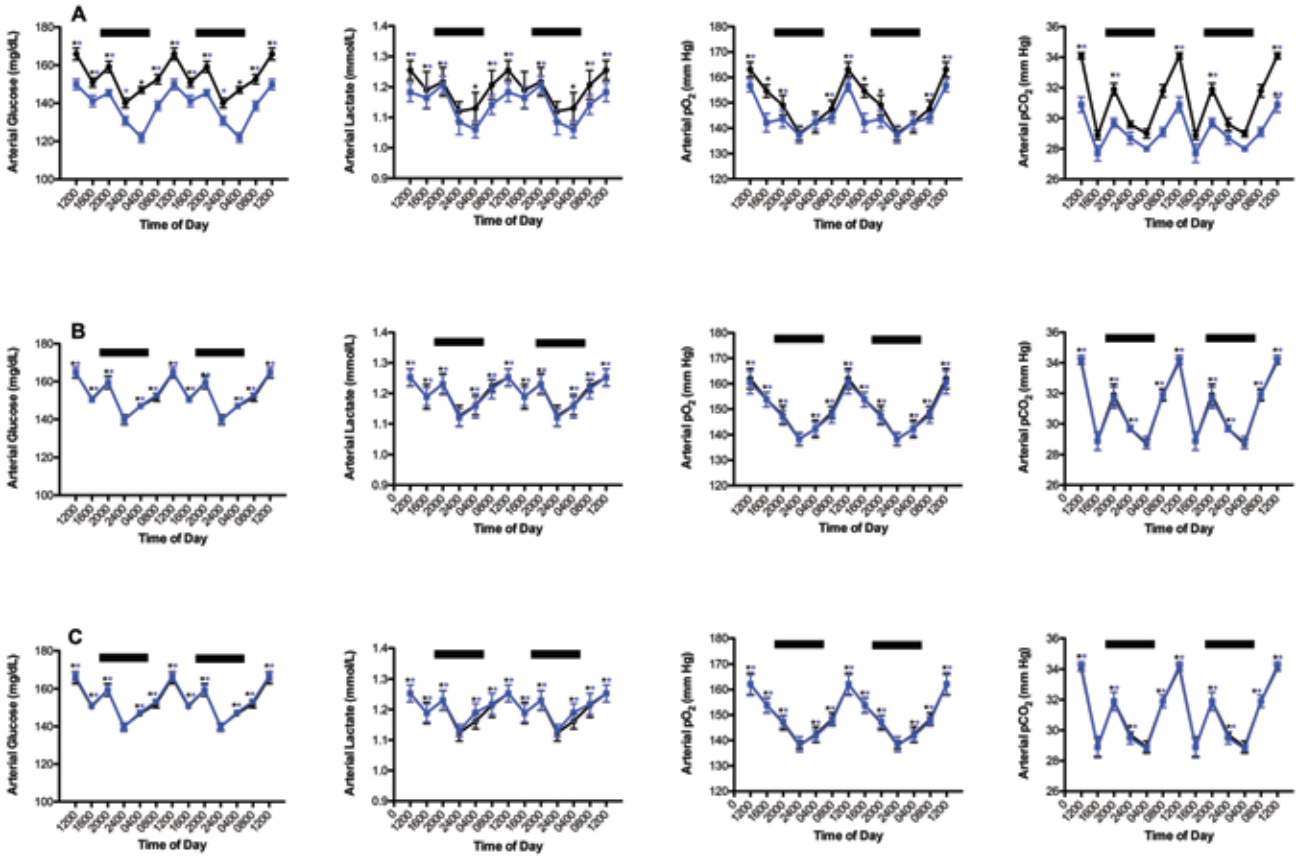

Figure 4. Circadian changes in the arterial blood glucose, lactate, pO_2, and pCO_2 levels of male and female (A) C3H, (B) C57BL/6, and (C) BALB/c mice maintained under either control (solid black circles) or experimental (solid blue squares) lighting conditions (mean ± 1 SD; n = 120 per group). Mice were exposed to dark-phase lighting conditions from 1800 to 0600 (dark bars). Data are plotted twice to better visualize rhythmicity. Rhythmicity analysis (Table 3) revealed robust and highly significant ($P < 0.0001$) rhythmic patterns for both control CWF and experimental bLAD groups but a significantly disrupted ($P < 0.05$) phase pattern for bLAD group animals of the C3H but not C57BL/6 or BALB/c strain. *, Value differs significantly ($P < 0.001$) between experimental and control conditions (Student t test).

mg/mL compared with 11.53 ± 0.15 mg/mL for males and 11.58 ± 0.15 mg/mL for females in the BALB/c strain, respectively. Circadian cycling was evident for both CWF and bLAD groups in all strains of mice, with a severely dampened amplitude during daytime (Table 3).

Arterial blood glucose, lactate, acid-gas levels. Figure 4 depicts the combined values for male and female 24-h rhythms in levels of arterial blood glucose, lactate, pO_2, and pCO_2 in C3H (Figure 4 A), C57BL/6 (Figure 4 B), and BALB/c (Figure 4 C) mice. Phase shifts were determined by comparing the peak values (acrophases) between the mice in bLAD (experimental) and CWF lighting regimens. A 'phase advance' was defined as a shift in a group peak level to an earlier time (for example, from 1600 to 1200), whereas a 'phase delay' was defined as a shift in a group to a later time (for example, from 0800 to 1200), as compared with control values. Daily rhythms for arterial glucose and lactate concentrations (Figure 4 A and B) were equivalent between CWF and bLAD groups for all strains, with peaks for both constituents occurring at 1200 and 2000 and bathyphase occurring between 2400 and 0400 (Table 3). In contrast to the C57BL/6 and BALB/c strains, however, the integrative mean over the 24-h day for C3H control mice was higher compared with that in the bLAD experimental group. C3H mice were the only strain that displayed significant differences in the arterial blood chemistries measured in the study; the average arterial blood glucose and lactate concentrations calculated over the 24-h day were 916 ± 3 mg/dL and 7.1 ± 0.1 mmol/L, respectively, for the control group and 828 ± 2 mg/dL and 6.84 ± 0.03 mmol/L, respectively, for the experimental group ($P < 0.0006$). The integrative mean arterial blood pO_2 and pCO_2 concentrations calculated over the 24-h day were 977 ± 3 mm Hg and 202 ± 1 mm Hg for the control group and 944 ± 2 mm Hg and 190 ± 0.3 mm Hg for the experimental group ($P < 0.007$). In C57BL/6 mice, the average arterial blood glucose and lactate concentrations calculated over the 24-h day were 996 ± 2 mg/dL and 7.8 ± 0.1 mmol/L for the control group and 997 ± 3 mg/dL and 7.81 ± 0.04 mmol/L for the experimental group. The integrative mean arterial blood pO_2 and pCO_2 concentrations calculated over the 24-h day were 974 ± 2 mm Hg and 202 ± 1 mm Hg for the control group and 970 ± 2 mm Hg and 202 ± 1 mm Hg for the experimental group. In BALB/c mice, the average arterial blood glucose and lactate concentrations calculated over the 24-h day were 998 ± 3 mg/dL and 7.80 ± 0.01 mmol/L for the control group and 1003 ± 3 mg/dL and 7.84 ± 0.01 mmol/L for the experimental group. The integrative mean arterial blood pO_2 and pCO_2 concentrations calculated over the 24-h day were 973 ± 2 mm Hg and 203 ± 1 mm Hg for the control group and 973.3 ± 1.1 mm Hg and 202.3 ± 0.6 mm Hg for the experimental group.

Arterial blood pH and O_2 saturation, remained relatively constant for both sexes of all strains of both CWF and bLAD

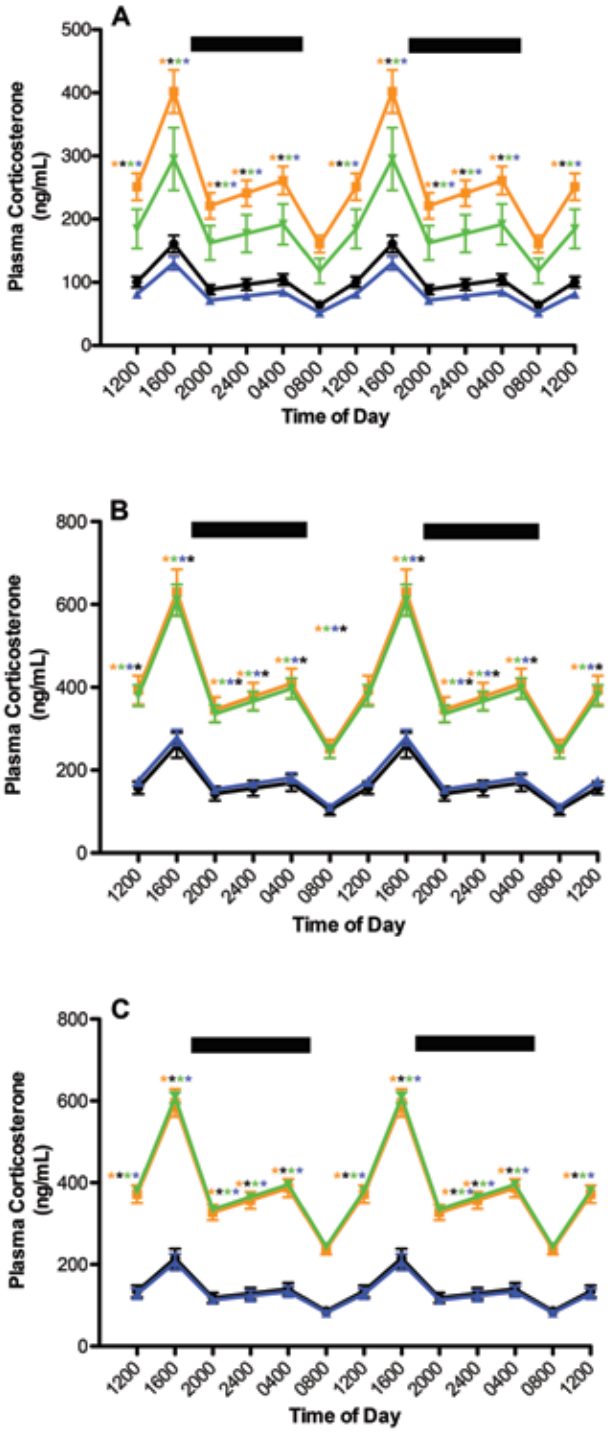

Figure 5. Circadian changes in plasma corticosterone in the arterial blood of (A) C3H, (B) C57BL/6, and (C) BALB/c mice maintained under either CWF control (male, solid black circles; female, solid amber squares) or experimental bLAD (male, solid blue triangles; female, solid green inverted triangles) lighting conditions. Data are plotted twice to better demonstrate rhythmicity. Dark bars represent dark-phase lighting conditions from 1800 to 0600. Rhythmicity analysis (Table 3) revealed robust and highly significant ($P < 0.0001$) rhythmic patterns under control conditions, with significant ($P < 0.05$) but disrupted rhythmic patterns under experimental conditions for corticosterone (*, $P < 0.001$) in C3H but not C57BL/6 and BALB/c mice.

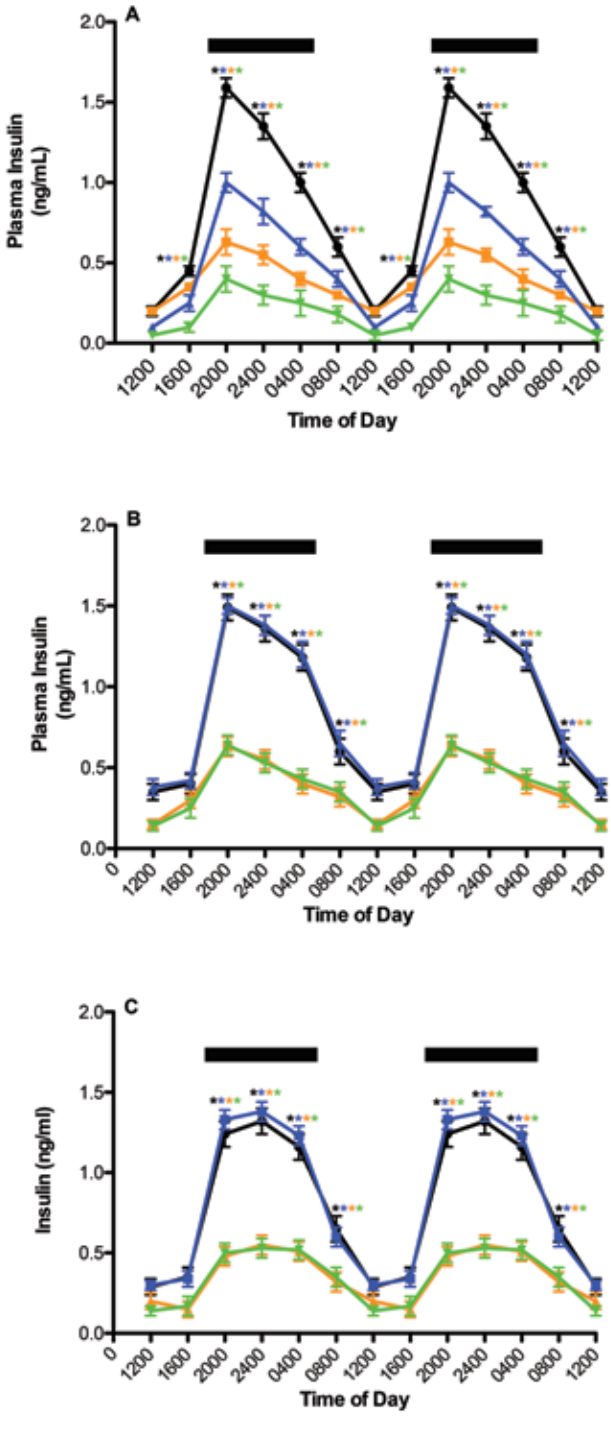

Figure 6. Circadian changes in plasma insulin in the arterial blood of (A) C3H, (B) C57BL/6, and (C) BALB/c mice maintained under either CWF control (male, solid black circles; female, solid amber squares) or experimental bLAD (male, solid blue triangles; female, solid green inverted triangles) lighting conditions. Data are plotted twice to better demonstrate rhythmicity. Mice were exposed to dark-phase lighting conditions from 1800 to 0600 (dark bars). Rhythmicity analysis (Table 3) revealed robust and highly significant ($P < 0.0001$) rhythmic patterns under control conditions, with significant ($P < 0.05$) but disrupted rhythmic patterns under experimental conditions for insulin (*, $P < 0.001$) in C3H but not C57BL/6 and BALB/c mice.

groups over the 24-h day, at 7.43% ± 0.17% and 99.2% ± 0.2%, respectively ($n = 360$). Cumulative mean arterial Hct values were 45.8% ± 0.20% for males and 44.0 ± 0.30% for females in the C3H strain, 51.7% ± 0.20% for males and 51.0% ± 0.30% for females in the C57BL/6 strain, and 45.7% ± 0.20% for males and 44.9% ± 0.20% for females in the BALB/c strain. Mean arterial Hgb

values (n = 60 per sex) were 15.7 ± 0.2 g/dL for males and 15.1 ± 0.1 g/dL for females in the C3H strain, 15.9 ± 0.20 g/dL for males and 16.3 ± 0.3 g/dL for females in the C57BL/6 strain, and 13.5 ± 0.2 g/dL for males and 14.7 ± 0.3 g/dL for females in the BALB/c strain.

Plasma measures of corticosterone, insulin, and leptin. Figure 5 depicts 24-h rhythms in concentrations of arterial blood plasma corticosterone in male and female C3H, C57BL/6, and BALB/c mice (Table 3). Plasma corticosterone levels revealed clear differences between the CWF and bLAD groups, with regard to integrative concentrations, and the amplitude of both the primary and secondary peaks was significantly ($P < 0.05$) lower in the bLAD group than in the CWF group, with the general trend following C57BL/6 > BALB/c > C3H (female > male). Values for arterial plasma corticosterone in all mouse strains of both groups began to increase after 1200 ($P < 0.05$), with a major peak value occurring at 1600 (secondary peak; $P < 0.05$) in the experimental and control groups, decreasing to a low value at 2000 ($P < 0.05$) for both CWF and bLAD groups in all strains and sexes. A second minor peak occurred in both CWF and bLAD groups at 0400 (but was higher in control CWF mice), decreasing to a nadir at 0800 for both groups. Integrated plasma corticosterone concentrations calculated over the 24-h day (male/female) in C57BL/6, BALB/c, and C3H strains, respectively, were 1069.5 ± 47.3 ng/mL for male mice and 2640.5 ± 114.2 ng/mL for female mice, 852.0 ± 37.5 ng/mL for male mice and 2462.5 ± 107.7 ng/mL for female mice, and 665.0 ± 29.2 ng/mL for male mice and 1663.5 ± 72.8 ng/mL for female mice in the CWF animals, as compared with 1153.5 ± 50.5 ng/mL for male mice and 2524.0. ± 110.5 ng/mL for female mice, 890.0 ± 39.0 ng/mL for male mice and 2515.5 ± 110.2 ng/mL for female mice, and 540.0 ± 20.2 ng/mL for male mice and 1221.5 ± 53.4 ng/mL for female mice, respectively, in bLAD animals.

Plasma concentrations of insulin (Figure 6) showed clear intergroup differences with regard to 24-h rhythms and integrative levels in male and female C3H, C57BL/6, and BALB/c mice (Table 3). Plasma insulin levels revealed clear differences between the CWF and bLAD groups, with regard to integrative concentrations, and the amplitude of both the primary and secondary peaks was significantly lower ($P < 0.05$) in the bLAD group than in the CWF group, with the general trend following C57BL/6 > C3H > BALB/c (male > female). Values for arterial plasma insulin in all mouse strains of both groups began to increase sharply after 1600 ($P < 0.05$), with a major peak value occurring at 2000 for both CWF and bLAD groups in all strains and sexes ($P < 0.001$), decreasing gradually throughout the night phase and into the light phase to a nadir at 1200 ($P < 0.001$). Integrated plasma insulin concentrations calculated over the 24-h day in C57BL/6, BALB/c, and C3H strains, respectively, were 5.56 ± 0.49 ng/mL for male mice and 2.43 ± 0.17 ng/mL for female mice, 5.16 ± 0.45 ng/mL for male mice and 2.31 ± 0.16 ng/mL for female mice, and 5.29 ± 0.53 ng/mL for male mice and 2.53 ± 0.16 ng/mL for female mice in the CWF groups, as compared with 5.72 ± 0.37 ng/mL for male mice and 2.41 ± 0.18 ng/mL for female mice, 5.33 ± 0.49 ng/mL for male mice and 2.28 ± 0.17 ng/mL for female mice, and 3.22 ± 0.34 ng/mL for male mice and 1.31 ± 0.13 ng/mL for female mice, respectively, in bLAD groups. Integrated plasma leptin concentrations calculated over the 24-h day in C57BL/6, C3H, and BALB/c mice, respectively, were 5.56 ± 0.49 ng/mL for male mice and 2.43 ± 0.17 ng/mL for female mice, 5.16 ± 0.45 ng/mL for male mice and 2.31 ± 0.16 ng/mL for female mice, and 5.29 ± 0.53 ng/mL for male mice and 2.53 ± 0.16 ng/mL for female mice in the CWF animals, as compared with 5.72 ± 0.37 ng/mL for male mice and

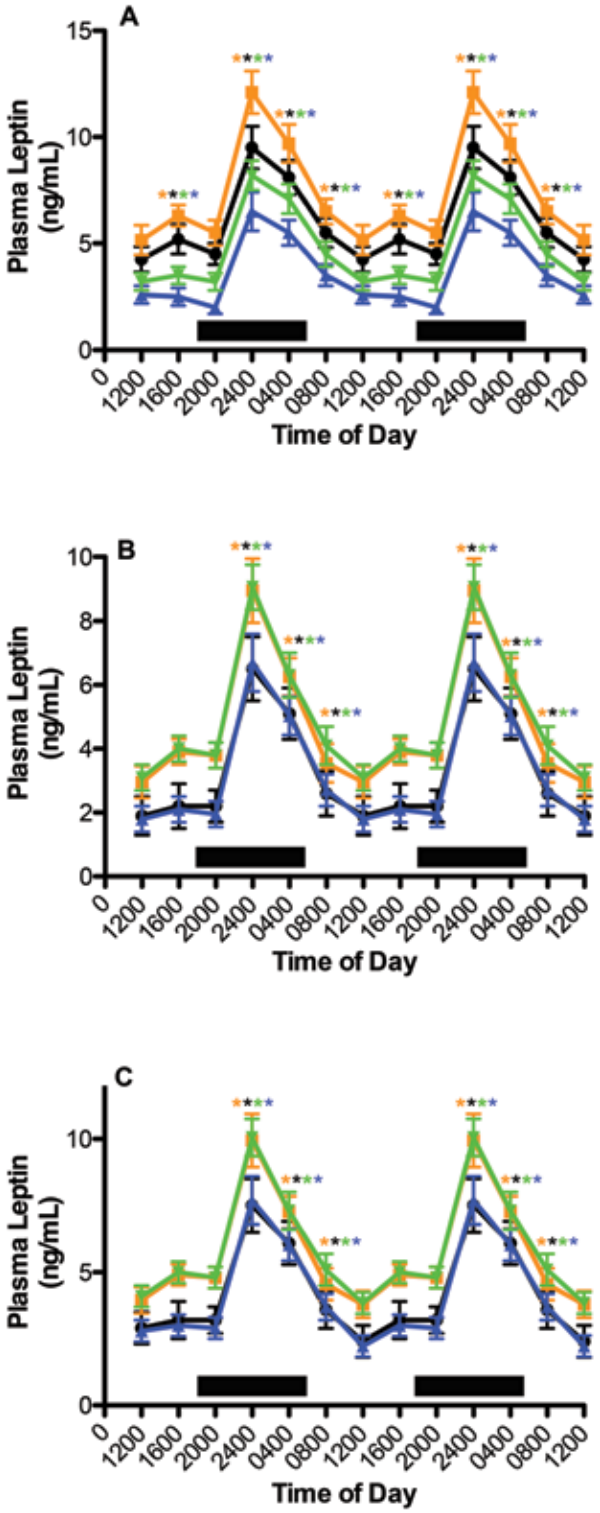

Figure 7. Circadian changes in plasma leptin in the arterial blood of (A) C3H, (B) C57BL/6, and (C) BALB/c mice maintained under either CWF control (male, solid black circles; female, solid amber squares) or experimental bLAD (male, solid blue triangles; female, solid green inverted triangles) lighting conditions. Data are plotted twice to better demonstrate rhythmicity. Black bars represent dark-phase lighting conditions from 1800 to 0600. Rhythmicity analysis (Table 3) revealed robust and highly significant ($P < 0.0001$) rhythmic patterns under control conditions, with significant ($P < 0.05$) but disrupted rhythmic patterns under experimental conditions for leptin (*, $P < 0.001$) in C3H but not C57BL/6 and BALB/c mice.

Table 4. Effects of CWF and bLAD lighting on animal organ wet weight (g) of liver, retroperitoneal fat pad (1), quadricep femoris muscle (1), heart, lung (2), kidney (2), gut, brain, testes (2), and ovary (2) tissues in C3H, C57BL/6, and BALB/c male and female mice.

	C3H				C57BL/6				BALB/c			
	CWF		bLAD		CWF		bLAD		CWF		bLAD	
Tissue	M	F	M	F	M	F	M	F	M	F	M	F
Liver	1.870 ± 0.038	1.650 ± 0.015[a]	1.728 ± 0.032[a,b]	1.502 ± 0.013[a-c]	1.606 ± 0.026[b,c,d]	1.466 ± 0.021[a,c,d,e]	1.512 ± 0.013[a-c,e,f]	1.368 ± 0.026[a-g]	1.610 ± 0.022[a-d,f,g,h]	1.472 ± 0.019[a-e,g,h,i]	1.506 ± 0.025[a-e,h,i]	1.350 ± 0.038[a-g,i,j,k]
Fat	0.060 ± 0.009	0.123 ± 0.008[a]	0.047 ± 0.006[a,b]	0.103 ± 0.004[a-c]	0.054 ± 0.006[b,d]	0.120 ± 0.006[a,c,d,e]	0.055 ± 0.008[b,d,f]	0.121 ± 0.004[a,c,d,e,g]	0.057 ± 0.010[b,d,f,h]	0.122 ± 0.007[a,c,d,e,g,i]	0.055 ± 0.005[b,d,f,h,i]	0.121 ± 0.002[a,c,d,e,g,i,k]
Muscle	0.179 ± 0.003	0.167 ± 0.002[a]	0.187 ± 0.002[a,b]	0.176 ± 0.002[b,c]	0.168 ± 0.001[a,c,d]	0.133 ± 0.002[a-e]	0.168 ± 0.001[a,c,d,f]	0.134 ± 0.002[a-e,g]	0.170 ± 0.001[a-h]	0.153 ± 0.001[a-i]	0.171 ± 0.001[a-h,j]	0.155 ± 0.001[a-i,k]
Heart	0.131 ± 0.001	0.115 ± 0.001[a]	0.124 ± 0.001[a,b]	0.112 ± 0.001[a-c]	0.211 ± 0.001[a-d]	0.172 ± 0.002[a-e]	0.212 ± 0.002[a-c,d,f]	0.173 ± 0.001[a-e,g]	0.151 ± 0.001[a-h]	0.122 ± 0.001[a,b,d-i]	0.151 ± 0.001[a,-h,j]	0.122 ± 0.002[a,b,d-i,k]
Lung	0.188 ± 0.001	0.180 ± 0.001[a]	0.179 ± 0.001[a,b]	0.175 ± 0.001[a-c]	0.191 ± 0.001[a-d]	0.181 ± 0.001[a,c,d,e]	0.191 ± 0.001[a-d,f]	0.181 ± 0.001[a,d,e,g]	0.191 ± 0.001[a-d,f,h]	0.180 ± 0.001[a,d,e,g,i]	0.191 ± 0.001[a-c,d,f,h,j]	0.179 ± 0.002[a,d,e,g,i,k]
Kidney	0.460 ± 0.002	0.276 ± 0.001[a]	0.412 ± 0.002[a,b]	0.251 ± 0.002[a-c]	0.424 ± 0.002[a-d]	0.266 ± 0.002[a-e]	0.425 ± 0.001[a-d,f]	0.267 ± 0.002[a-e,g]	0.444 ± 0.002[a-g]	0.285 ± 0.001[a-i]	0.445 ± 0.001[a-h,j]	0.285 ± 0.002[a-i,k]
Gut	1.219 ± 0.007	1.192 ± 0.0.009[a]	1.116 ± 0.007[a,b]	1.085 ± 0.007[a-c]	1.192 ± 0.008[a,c,d]	1.165 ± 0.006[a-e]	1.194 ± 0.005[a,c,d,f]	1.166 ± 0.006[a-e,g]	1.200 ± 0.005[a-d,f,h]	1.180 ± 0.003[a-i]	1.201 ± 0.008[a-d,f,h,j]	1.181 ± 0.005[a-i,k]
Brain	0.421 ± 0.002	0.425 ± 0.002[a]	0.416 ± 0.002[a,b]	0.420 ± 0.001[b,c]	0.416 ± 0.001[a,b,d]	0.421 ± 0.002[a-c,e]	0.413 ± 0.002[a-c,f]	0.419 ± 0.001[b,e,g]	0.376 ± 0.002[a-h]	0.386 ± 0.001[a-i]	0.371 ± 0.001[a-j]	0.383 ± 0.001[a-i,k]
Testes	0.160 ± 0.020	_	0.134 ± 0.024[a]	_	0.233 ± 0.020[a,c]	_	0.230 ± 0.030[a,c]	_	0.180 ± 0.023[a,c,e,g]	_	0.183 ± 0.019[a,c,e,g]	_
Ovary	_	0.0051 ± 0.0008	_	0.0044 ± 0.0006[b]	_	0.0073 ± 0.0027[b,d]	_	0.0074 ± 0.0019[b,d]	_	0.0056 ± 0.0017[d,f,h]	_	0.0056 ± 0.0014[d,f,h]

Values represent means ± 1 SD (n = 30/group; that is, 30 males and 30 females in each lighting environment per strain)
[a]$P < 0.05$ compared with value for C3H mice in male CWF control group.
[b]$P < 0.05$ compared with value for C3H mice in female CWF control group.
[c]$P < 0.05$ compared with value for C3H mice in male bLAD experimental group.
[d]$P < 0.05$ compared with value for C3H mice in female bLAD experimental group.
[e]$P < 0.05$ compared with value for C57BL/6 mice in male CWF control group.
[f]$P < 0.05$ compared with value for C57BL/6 mice in female CWF control group.
[g]$P < 0.05$ compared with value for C57BL/6 mice in male bLAD experimental group.
[h]$P < 0.05$ compared with value for C57BL/6 mice in female bLAD experimental group.
[i]$P < 0.05$ compared with value for BALB/c mice in male CWF control group.
[j]$P < 0.05$ compared with value for BALB/c mice in female CWF control group.
[k]$P < 0.05$ compared with value for BALB/c mice in male bLAD experimental group.

2.41 ± 0.18 ng/mL for female mice, 5.33 ± 0.49 ng/mL for male mice and 2.28 ± 0.17 ng/mL for female mice, and 3.22 ± 0.34 ng/mL for male mice and 1.31 ± 0.13 ng/mL for female mice, respectively, in bLAD animals.

Plasma concentrations of leptin (Figure 7) revealed clear intergroup differences with regard to 24-h rhythms (Table 3) and integrative levels in male and female C3H, C57BL/6, and BALB/c mice. For male and female mice in groups (C3H > BALB/c > C57BL/6) in either CWF or bLAD lighting environments (female > male), values for arterial plasma leptin began to increase 2 h after the onset of the dark phase ($P < 0.05$), with peak levels occurring at 2400 and gradually decreasing to a nadir at 1200 ($P < 0.05$) in controls. Integrated plasma leptin concentrations calculated over the 24-h day in C3H, BALB/c, and C57BL/6 strains, respectively, were 39.18 ± 2.02 ng/mL for male mice and 47.84 ± 2.60 ng/mL for female mice, 27.45 ± 1.87 ng/mL for male mice and 37.23 ± 2.18 ng/mL for female mice, and 21.45 ± 1.79 ng/mL for male mice and 30.88 ± 2.15 ng/mL for female mice in the CWF animals, as compared with 23.90 ± 1.69 ng/mL for male mice and 31.30 ± 2.04 ng/mL for female mice, 26.95 ± 1.99 ng/mL for male mice and 38.15 ± 2.15 ng/mL for female mice, and 21.18 ± 1.89 ng/mL for male mice and 31.90 ± 2.11 ng/mL for female mice, respectively, in bLAD animals. Again, circadian cycling for all 3 neurohormones was evident in all strains, with the general trend toward high levels near the end of the light phase and markedly dampened during dark phase (Table 3).

Major tissue organ weight, total fatty acid, protein, and cAMP content. Table 4 depicts mean weights (in grams) of excised organs (liver, left retroperitoneal fat pad, left quadricep femoris muscle, heart, lungs, kidneys, small intestine, brain, testes, and ovaries) at the time of harvest (age, 12 wk) from male and female C3H, C57BL/6, and BALB/c mice maintained in either CWF control or bLAD experimental groups. With the exception of the fat pad and brain, organs collected from male mice were significantly ($P < 0.05$) heavier than those of female mice, proportional to the final body weights in these animals. Overall, normalizing for sex, strain, and final body weights, the combined (male and female) weight for all 10 major organs in the CWF control group was 7.89% ± 0.01% and 7.96 ± 0.01% higher, respectively, than that of the bLAD experimental group in the C3H mouse strain ($P < 0.05$). This was not the case with either the C57BL/6 or BALB/c strains, in which this value did not differ significantly between lighting conditions. In general, organ weight was proportional to the final body weight (male > female) for each strain (C3H > C57BL/6 > BALB/c), and the cumulative tissue mass for all tissues collected were 4.69 ± 0.01 g for male mice and 4.13 ± 0.004 g for female mice, 4.49 ± 0.01 g for male mice and 3.93 ± 0.01 g for female mice, and 4.00 ± 0.01 g for male mice and 3.91 ± 0.004 g for female mice, respectively, in the control CWF group, as compared with 4.34 ± 0.01 g for male mice and 3.83 ± 0.004 g for female mice; 4.40 ± 0.01 g for male mice and 3.84 ± 0.01 g for female mice, and 4.27 ± 0.01 g

Table 5. Effects of CWF and bLAD daytime lighting on total fatty acid levels (mg/g tissue) of liver, fat, skeletal muscle, heart, lung, kidney, gut, brain, testes, and ovary tissues in C3H, C57BL/6, and BALB/c male and female mice

	C3H				C57BL/6				BALB/c			
	CWF		bLAD		CWF		bLAD		CWF		bLAD	
Tissue	M	F	M	F	M	F	M	F	M	F	M	F
Liver	25.60 ± 0.65	19.92 ± 0.38[a]	18.15 ± 0.95[a,b]	15.28 ± 0.83[a-c]	24.39 ± 1.27[b-d]	20.90 ± 1.09[a,c-e]	23.44 ± 1.22[b-d]	20.81 ± 1.09[a,c-e]	26.71 ± 1.39[b-d,f]	21.78 ± 1.13[a-e,g]	24.77 ± 1.29[b-f]	20.43 ± 1.06[a-h]
Fat	185.31 ± 13.19	85.56 ± 4.42[a]	125.92 ± 7.44[a,b]	57.03 ± 4.48[a-c]	139.80 ± 11.55[a-d]	100.40 ± 7.37[a,c-e]	142.87 ± 7.13[a-d]	100.35 ± 6.97[a-e]	117.34 ± 7.27[a-d,f]	100.49 ± 5.12[a-,g]	117.20 ± 7.26[b-f]	100.17 ± 7.72[a-h]
Muscle	30.31 ± 1.99	24.72 ± 1.77[a]	21.68 ± 1.80[a,b]	17.68 ± 1.46[a-c]	28.88 ± 2.06[a-d]	25.43 ± 1.81[a-e]	31.31 ± 2.23[a-e]	27.09 ± 1.93[a-e]	28.05 ± 1.50[a-e]	24.55 ± 1.88[a-f]	28.70 ± 2.29[a-f]	25.63 ± 1.59[a-g]
Heart	8.72 ± 0.62	6.14 ± 0.44[a]	6.10 ± 0.51[a,b]	4.78 ± 0.40[a-c]	6.32 ± 0.37[a-d]	6.31 ± 0.45[a-d]	6.44 ± 0.46[a-d]	6.32 ± 0.45[a-d]	7.16 ± 0.50[a-f]	5.47 ± 0.39[a-g]	7.19 ± 0.51[a-f]	6.33 ± 0.99[a-g]
Lung	18.56 ± 1.33	14.16 ± 1.01[a]	12.15 ± 0.82[a,b]	9.67 ± 0.79[a-c]	15.94 ± 1.14[a-d]	14.70 ± 1.05[a-e]	13.51 ± 0.96[a-e]	11.06 ± 0.79[a-e]	15.62 ± 1.11[a-e]	12.78 ± 0.91[a-f]	13.77 ± 0.83[a-f]	12.33 ± 0.88[a-g]
Kidney	27.01 ± 1.92	17.29 ± 1.23[a]	16.56 ± 1.04[a,b]	11.91 ± 0.81[a-c]	24.60 ± 1.75[b-d]	15.92 ± 1.14[a,c-e]	25.12 ± 1.22[b-d]	16.90 ± 1.17[a,c-e]	19.60 ± 1.40[b-d,f]	18.96 ± 1.35[a-e,g]	19.67 ± 1.40[b-f]	17.25 ± 1.23[a-h]
Gut	27.70 ± 2.01	19.65 ± 1.40[a]	17.85 ± 1.46[a,b]	15.95 ± 1.28[a-c]	21.85 ± 2.20[b-d]	16.37 ± 0.55[a,c-e]	22.11 ± 1.58[b-d]	16.76 ± 1.20[a,c-e]	23.91 ± 2.24[b-d,f]	19.95 ± 1.71[a-e,g]	24.95 ± 2.16[b-f]	19.00 ± 2.23[a-h]
Brain	20.96 ± 1.45	19.52 ± 1.57[a]	17.58 ± 1.46[a,b]	14.68 ± 1.37[a,b,c]	21.07 ± 1.50[b,c,d]	16.81 ± 1.20[a,c-e]	15.33 ± 1.09[b-d]	13.99 ± 1.02[a,c-e]	25.96 ± 1.85[b-d,f]	22.58 ± 1.61[a-e,g]	20.70 ± 1.48[b-f]	20.97 ± 1.78[c-g]
Testes	58.72 ± 4.19	_	48.25 ± 3.45[a]	_	57.87 ± 4.16	_	57.51 ± 4.05[c]	_	64.86 ± 4.63[a,c,e]	_	65.05 ± 4.64[a,c,e]	_
Ovary	_	43.98 ± 3.14	_	33.87 ± 1.88[b]	_	43.59 ± 3.11[b,d]	_	43.47 ± 3.10[d]	_	43.67 ± 3.12[d]	_	43.58 ± 4.19[d]

Values represent means ± 1 SD (n = 30/group; that is, 30 males and 30 females in each lighting environment per strain)
[a]$P < 0.05$ compared with value for C3H mice in male CWF control group.
[b]$P < 0.05$ compared with value for C3H mice in female CWF control group.
[c]$P < 0.05$ compared with value for C3H mice in male bLAD experimental group.
[d]$P < 0.05$ compared with value for C3H mice in female bLAD experimental group.
[e]$P < 0.05$ compared with value for C57BL/6 mice in male CWF control group.
[f]$P < 0.05$ compared with value for C57BL/6 mice in female bLAD experimental group
[g]$P < 0.05$ compared with value for BALB/c mice in male CWF control group.
[h]$P < 0.05$ compared with value for BALB/c mice in male experimental control group.

for male mice and 3.78 ± 0.01 g for female mice, respectively, in the experimental bLAD group.

The TFA content of the major metabolic organs of mice in the control CWF and experimental bLAD groups is depicted in Table 5 (C3H > C57BL/6 > BALB/c). TFA levels in liver, adipose (fat), hindlimb skeletal muscle, heart, lung, kidney, small intestine, brain, and testes or ovary tissues were significantly ($P < 0.001$) higher in mice of the CWF group (male > female) compared with those of the bLAD group (male > female) only in the C3H strain. Overall, TFA content was highest in fat tissue for all strains and lighting environments (males, 40.9% ± 1.1%; females, 37.2 ± 0.9%) and lowest in heart tissue (males, 2.1% ± 0.1%; females, 2.4% ± 0.2%). The mean of combined tissue TFA levels for male and female mice in the CWF control group was 41.7% ± 1.2% and 38.8% ± 1.4% higher ($P < 0.001$) than that of the male and female mice in the bLAD experimental group, respectively. In contrast, the mean of combined tissue TFA levels for male and female mice in both the C57BL/6 and BALB/c mouse strains in the CWF control compared with bLAD group were nearly identical and not significantly different.

The protein content of the major metabolic organs of mice in the control CWF and experimental bLAD groups is listed in Table 6 (C3H > C57BL/6 > BALB/c). The combined protein content values for all tissues in C3H, C57BL/6, and BALB/c mice in bLAD compared with CWF light groups were 1049.0 g for male mice and 835.0 g for female mice and 843.4 for male mice and 681.8 g for female mice; 943.7 g for male mice and 804.1 g for female mice and 1099.6 g for male mice and 901.6 g for female mice; and 972.8 g for male mice and 798.0 g for female mice and 1151.7g for male mice and 866.0 g for female mice, respectively. Tissue protein levels followed the general trend of skeletal muscle > liver > lung > heart > kidney > brain > fat > gut > testes > ovary tissues for all groups and were significantly ($P < 0.001$) higher in mice of the bLAD group (male > female) compared with those of the CWF group (male > female) only in the C3H strain in males (24.4% ± 0.5%) and females (22.5% ± 0.4%), respectively. Conversely, in the C57BL/6 and BALB/c strains, total tissue protein content was lower in mice maintained in bLAD compared with CWF by 14.2% ± 0.5% for male mice and 10.8% ± 0.3% for female mice and 15.5% ± 0.6% for male mice and 7.9% ± 0.3% for female mice, respectively. Overall, as a percentage of total protein content, skeletal muscle tissue was highest for all strains and lighting environments (males, 30.0% ± 1.8%; females, 28.7% ± 2.5%), respectively, and lowest in intestinal tissue (males, 3.8% ± 1.1%; females, 3.8% ± 0.7%).

We examined whether cAMP, a derivative of the energy molecule ATP and essential in glucose and lipid metabolism and signal transduction, exhibited differences in the 2 most important metabolic tissues, skeletal muscle (Figure 8) and liver tissue (Figure 9). Circadian rhythms of cAMP levels were most pronounced in the C3H mouse strain compared with the C57BL/6 and BALB/c strains, having a similar profile for both male and female mice (Table 3). All 3 strains demonstrated an abrupt rise in skeletal muscle and liver cAMP levels in late light phase (1600) followed by a gradual decrease throughout the dark phase. Peak levels (1600) were significantly ($P < 0.001$) higher by 69.5% ± 4.5% and 89.3 ± 3.8%, respectively, for skeletal muscle and liver tissue in C3H mice maintained in bLAD

Table 6. Effects of cool white fluorescent and blue-enriched LED daytime lighting on tissue protein levels (mg/g tissue) of liver, fat, skeletal muscle, heart, lung, kidney, gut, brain, testes, and ovary tissues in C3H, C57BL/6, and BALB/c male and female mice.

	C3H				C57BL/6				BALB/c			
	CWF		bLAD		CWF		bLAD		CWF		bLAD	
Tissue	M	F	M	F	M	F	M	F	M	F	M	F
Liver	111.11 ± 6.51	108.00 ± 5.83[a]	153.05 ± 8.56[a,b]	151.70 ± 8.32[a,b]	167.35 ± 7.11[a-d]	149.33 ± 10.93[a,c-e]	153.05 ± 8.10[a,b,e]	125.83 ± 9.14[a-g]	169.58 ± 7.27[a-d,f-h]	155.35 ± 7.73[a,b,e,h]	160.26 ± 6.91[b-d,f,g,h]	146.84 ± 8.34[a,b,e,h,i]
Fat	54.73 ± 2.19	64.06 ± 3.02[a]	70.89 ± 3.27[a,b]	75.86 ± 3.35[a,b]	77.67 ± 3.68[a,b]	59.68 ± 2.66[a-e]	69.31 ± 2.37[a,d-g]	59.46 ± 3.11[c-eg]	86.08 ± 2.91[a-h]	49.88 ± 2.11[a-h]	72.09 ± 5.10[a,b,f,I,j]	50.53 ± 2.44[b-i,k]
Muscle	271.42 ± 12.99	224.20 ± 10.80[a]	314.44 ± 11.77[a,b]	251.54 ± 9.46[a,b,c]	284.98 ± 12.03[b-d]	248.20 ± 8.69[a-c,e]	278.14 ± 11.57[b-d,f]	232.04 ± 11.73[a-e,g]	294.42 ± 11.48[a-h]	259.00 ± 12.22[a-c,e,g-i]	281.86 ± 10.28[a-d,f,h,j]	242.86 ± 10.79[a-e,g,i,j,k]
Heart	83.28 ± 2.88	59.16 ± 2.97[a,b]	105.90 ± 5.22[a,b]	75.32 ± 3.08[a-c]	152.00 ± 6.44[a-d]	96.32 ± 4.21[a-e]	129.12 ± 5.72[a-f]	87.98 ± 3.63[a-d]	159.70 ± 5.95[a-d,f-h]	105.28 ± 5.44[a,b,d-i]	138.70 ± 6.34[a-h,j]	92.72 ± 4.20[a-e,g,h,i,k]
Lung	89.36 ± 3.94	59.66 ± 3.02[a]	101.04 ± 6.21[a]	67.50 ± 3.77[a-c]	134.60 ± 5.99[a-d]	97.00 ± 4.04[a,b,d,e]	72.58 ± 3.66[a-c,e,f]	72.58 ± 3.66[a-f]	134.72 ± 3.92[a-d,f,g-h]	75.32 ± 3.67[a-f,i]	88.74 ± 3.38[b-j]	67.82 ± 3.81[a-c,e,f,i,j,k]
Kidney	82.09 ± 1.92	46.24 ± 3.23[a]	101.85 ± 6.14[a,b]	58.54 ± 2.67[a-c]	100.93 ± 4.75[a,b,d]	96.20 ± 2.4[a,b,d]	100.55 ± 4.97[b-d]	84.14 ± 3.17[b,-g]	96.13 ± 4.40[a,b,d,h]	78.30 ± 3.35[a-e,g-i]	87.31 ± 4.40[a-g,I,j]	74.97 ± 3.23[a-g,h,i,k]
Gut	35.56 ± 3.07	24.50 ± 1.40[a]	45.24 ± 2.46[a,b]	37.66 ± 1.28[a-c]	45.38 ± 2.27[a,b,d]	43.02 ± 3.10[a,b,d]	21.14 ± 1.29[b-f]	32.84 ± 1.66[b-g]	61.28 ± 2.27[a-h]	27.72 ± 1.79[a,c-i]	26.48 ± 2.16[a,c-f,h,i]	22.76 ± 1.15[a,c-f,h,i,-k]
Brain	76.62 ± 2.75	52.57 ± 2.68[a]	89.92 ± 3.46[a,b]	58.91 ± 2.41[a-c]	80.66 ± 3.50[a-d]	76.06 ± 3.33[b-d]	76.62 ± 3.09[b-e]	71.65 ± 3.10[b-e]	82.71 ± 4.08[b-d,f-h]	58.16 ± 2.61[a-c,e,g-i]	69.35 ± 3.48[a-g,i,j]	53.94 ± 2.18[a,c-i,k]
Testes	39.22 ± 2.83	_	66.62 ± 3.11[a]	_	56.06 ± 3.04[a,c]	_	43.14 ± 2.12[c,d]	_	68.00 ± 3.22[a,e,g]	_	48.10 ± 2.06[a,c,e]	_
Ovary	_	43.44 ± 3.25	_	57.92 ± 2.88[b]	_	35.80 ± 1.94[b,e]	_	37.56 ± 2.06[a,d]	_	56.92 ± 2.77[b,f,h,j]	_	45.52 ± 2.03[d,f,h,j]

Values represent means ± 1 SD (n = 30/group; that is, 30 males and 30 females in each lighting environment per strain)
[a]$P < 0.05$ compared with value for C3H mice in male CWF control group.
[b]$P < 0.05$ compared with value for C3H mice in female CWF control group.
[c]$P < 0.05$ compared with value for C3H mice in male bLAD experimental group.
[d]$P < 0.05$ compared with value for C3H mice in female bLAD experimental group.
[e]$P < 0.05$ compared with value for C57BL/6 mice in male CWF control group.
[f]$P < 0.05$ compared with value for C57BL/6 mice in female CWF control group.
[g]$P < 0.05$ compared with value for C57BL/6 mice in male bLAD experimental group.
[h]$P < 0.05$ compared with value for C57BL/6 mice in female bLAD experimental group.
[i]$P < 0.05$ compared with value for BALB/c mice in male CWF control group.
[j]$P < 0.05$ compared with value for BALB/c mice in female CWF control group.
[k]$P < 0.05$ compared with value for BALB/c mice in male bLAD experimental group.

compared with CWF controls. In contrast, peak cAMP levels in these tissues rose minimally, but were significantly ($P < 0.05$) higher by 5.9% ± 0.5% and 0.5% ± 0.03%, respectively, in C57BL/6 and BALB/c mice maintained as CWF controls compared with bLAD animals. Levels of cAMP for all strains and sexes of mice in all lighting environments remained consistently above 0.4 ng/g tissue over the course of the 24-h day. The integrative means for cAMP levels in skeletal muscle over a 24-h day were significantly ($P < 0.001$) higher in C3H male and female mice maintained in bLAD (7.45 nmol/g and 6.88 nmol/g, respectively) compared with CWF controls (6.39 nmol/g and 5.92 nmol/g, respectively). Such was not the case for C57BL/6 male and female mice maintained in bLAD (7.57 nmol/g and 7.91 nmol/g, respectively) compared with CWF controls (7.54 nmol/g and 7.86 nmol/g, respectively) or BALB/c male and female mice maintained in bLAD (7.09 nmol/g and 6.51 nmol/g, respectively) compared with CWF controls (7.08 nmol/g and 6.48 nmol/g, respectively). The integrative means for cAMP levels in liver tissue over a 24-h day were significantly ($P < 0.001$) higher in C3H male and female mice maintained in bLAD (3.02 nmol/g and 2.97 nmol/g, respectively) compared with CWF controls (2.14 nmol/g and 2.15 nmol/g respectively) but were not significantly different for C57BL/6 male and female mice maintained in bLAD (4.07 nmol/g and 4.06 nmol/g, respectively) compared with CWF controls (4.04 nmol/g and 4.06 nmol/g, respectively) or for BALB/c male and female mice maintained in bLAD (2.73 nmol/g and 2.72 nmol/g, respectively) compared with CWF controls (2.72 nmol/g and 2.70 nmol/g, respectively).

Tritiated thymidine incorporation into tissue DNA and DNA content. We next assessed whether mouse tissues exhibited differences in [^{3}H]thymidine uptake and incorporation into DNA, an index of cell proliferation, as a result of daytime bLAD exposure. Incorporation of [^{3}H]thymidine incorporation into various tissues of these mouse strains in the control CWF and experimental bLAD groups is listed in Table 7. Cumulative uptake and incorporation values over a 24-h day for all major tissues in C3H, C57BL/6, and BALB/c strains of mice in bLAD compared with CWF light groups were, respectively, 238.34 ± 0.28 disintegrations per minute (dpm)/g for male mice and 221.73 ± 0.14 dpm/g for female mice; 230.50 ± 0.16 dpm/g for male mice and 216.3 ± 0.15 dpm/g for female mice; and 233.55 ± 0.15 dpm/g for male mice and 216.73 ± 0.14 dpm/g for female mice, compared with 230.01 ± 0.18 dpm/g for male mice and 218.23 ± 0.14 dpm/g for female mice; 227.00 ± 0.19 dpm/g for male mice and 214.40 ± 0.16 dpm/g for female mice; and 233.41 ± 0.17 dpm/g for male mice and 224.12 ± 0.12 dpm/g for female mice ($P < 0.001$). Tissue [^{3}H]thymidine uptake and incorporation values followed the general trend of skeletal muscle > heart > liver > kidney > lung > brain > gut > fat > urogenital tissues > fat for all groups in all strains. Skeletal muscle and liver, the 2 most metabolically important tissues investigated in this study, revealed

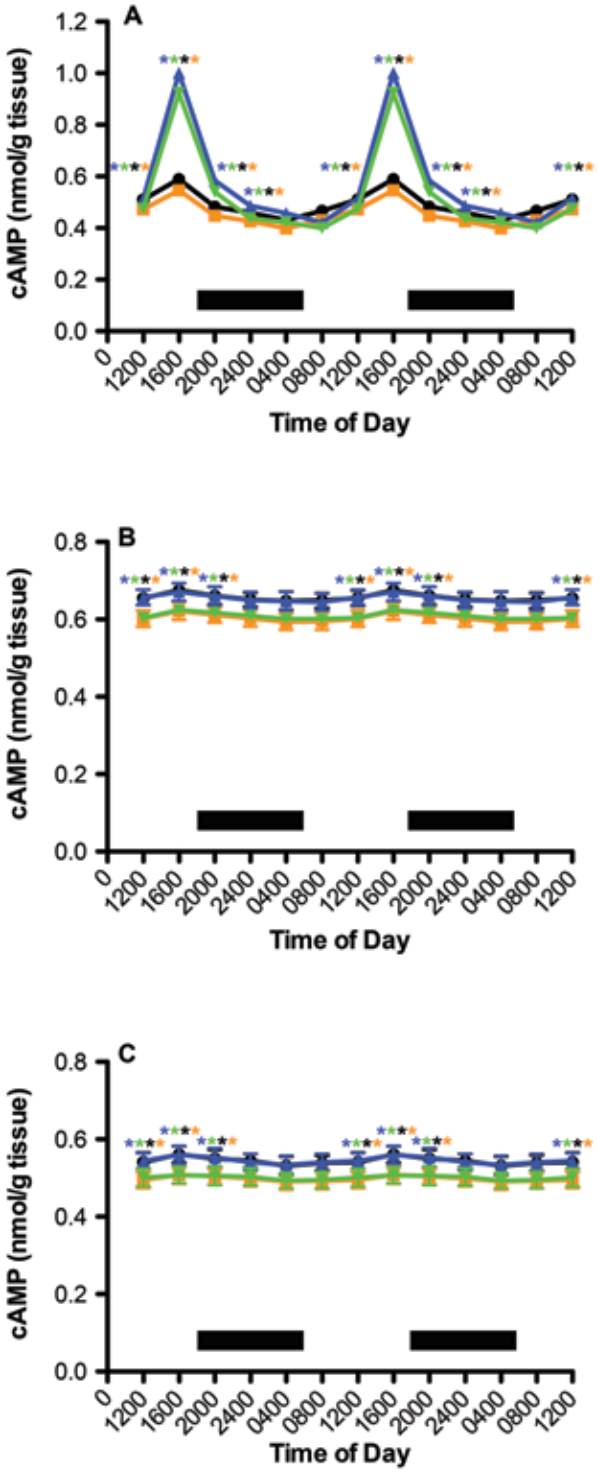

Figure 8. Circadian alterations in skeletal muscle cAMP levels (nmol/g) in (A) C3H, (B) C57BL/6, and (C) BALB/c mice maintained under either CWF control (male, solid black circles; female, solid amber squares) or experimental bLAD (male, solid blue triangles; female, solid green inverted triangles) lighting conditions. Data are plotted twice to better demonstrate rhythmicity. Dark bars represent dark-phase lighting conditions from 1800 to 0600. Rhythmicity analysis revealed robust and highly significant ($P < 0.0001$) rhythmic patterns under control conditions, with significant ($P < 0.05$) but disrupted rhythmic patterns under experimental conditions for skeletal muscle cAMP levels (*, $P < 0.001$) in C3H but not C57BL/6 and BALB/c mice.

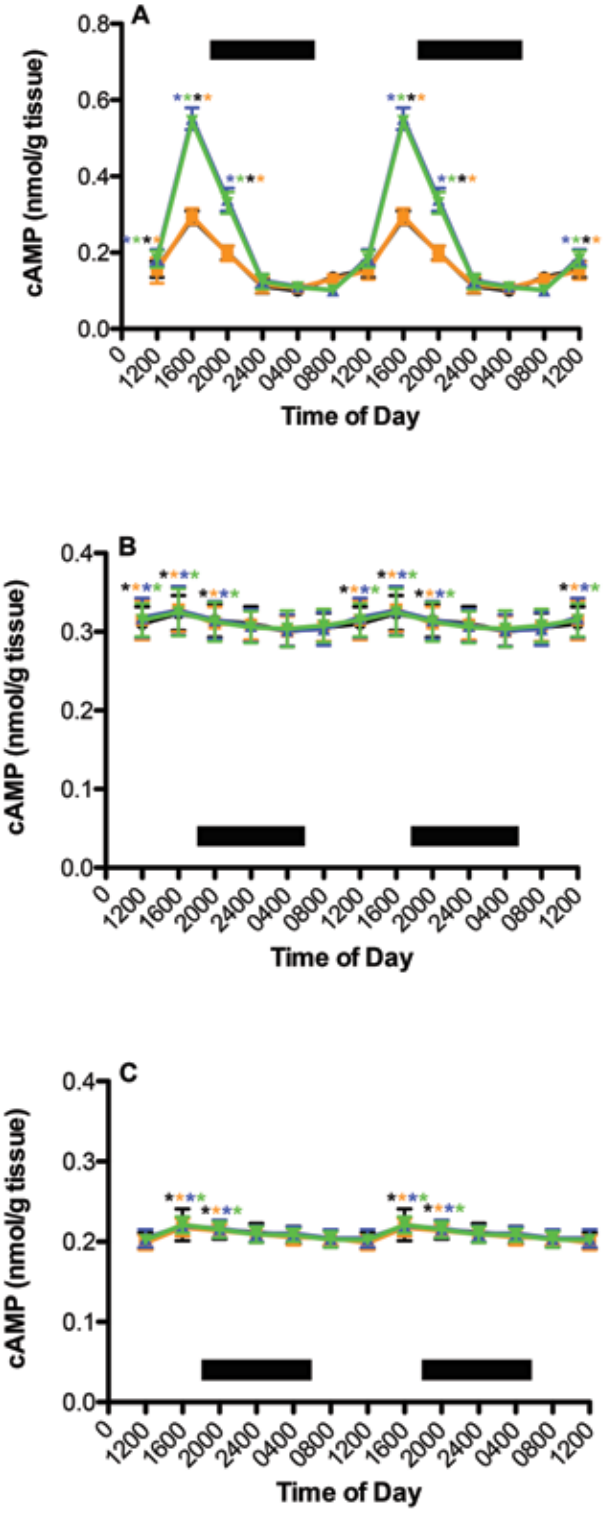

Figure 9. Circadian alterations in liver cAMP levels (nmol/g), in (A) C3H, (B) C57BL/6, and (C) BALB/c mice maintained on either CWF control (male, solid black circles; female, solid amber squares) or experimental bLAD (male, solid blue triangles; female, solid green inverted triangles) lighting conditions. Data are plotted twice to better demonstrate rhythmicity. Dark bars represent dark-phase lighting conditions from 1800 to 0600. Concentrations with asterisks are different ($P < 0.05$) from those without asterisks.

Table 7. Effects of cool white fluorescent and blue-enriched LED daytime lighting on [3H]Thymidine incorporation into tissue DNA in dpms/µg DNA of liver, fat, skeletal muscle, heart, lung, kidney, gut, brain, testes, and ovary tissues in C3H, C57BL/6, and BALB/c male and female mice.

	C3H				C57BL/6				BALB/c			
	CWF		bLAD		CWF		bLAD		CWF		bLAD	
Tissue	M	F	M	F	M	F	M	F	M	F	M	F
Liver	27.49 ± 0.17	27.06 ± 0.11[a]	26.11 ± 0.10[a,b]	25.89 ± 0.08[a-c]	28.09 ± 0.14[a-d]	27.82 ± 0.12[a-e]	28.19 ± 0.09[a-d,f]	28.02 ± 0.10[a-d,f]	28.21 ± 0.06[a-d,f]	28.03 ± 0.09[a-d,f]	28.16 ± 0.11[a-d,f,j]	27.98 ± 0.12[a-e]
Fat	2.82 ± 0.03	2.51 ± 0.02[a]	1.99 ± 0.01[a,b]	1.69 ± 0.02[a-c]	2.95 ± 0.08[a-d]	2.81 ± 0.01[c-e]	2.87 ± 0.09[b-d]	2.79 ± 0.05[c-e]	2.86 ± 0.06[c,d,h]	2.81 ± 0.02[c-h]	2.90 ± 0.05[b-d,h]	2.81 ± 0.03[b-d]
Muscle	52.56 ± 0.21	49.48 ± 0.29[a]	68.70 ± 0.19[a,b]	57.42 ± 0.28[a-c]	46.43 ± 0.30[a-c]	43.18 ± 0.29[a-d]	46.57 ± 0.17[a-d,f]	43.29 ± 0.24[a-e,g]	50.74 ± 0.26[a- h]	48.99 ± 0.16[a-e,g-i]	50.55 ± 0.29[a-h,j]	48.73 ± 0.25[a-h,k]
Heart	43.51 ± 0.25	39.98 ± 0.27[a]	46.62 ± 0.21[a,b]	43.03 ± 0.30[a-c]	44.72 ± 0.41[b-d]	40.22 ± 0.28[a,c-e]	45.08 ± 0.27[a-e]	40.68 ± 0.25[a-e,g]	46.04 ± 0.36[a,b,d-h]	44.96 ± 0.20[a-c,f-i]	45.94 ± 0.31[a-h,j]	45.02 ± 0.26[a-f,h,I,k]
Lung	25.69 ± 0.27	25.03 ± 0.19[a]	23.22 ± 0.25[a,b]	22.87 ± 0.14[a-c]	25.04 ± 0.16[a,c,d]	24.88 ± 0.05[a,c,d]	26.11 ± 0.23[a-f]	25.98 ± 0.14[b-g]	25.04 ± 0.14[a,c,d,g,h]	25.10 ± 0.16[a,b,d,g]	25.31 ± 0.15[b-d,g]	25.22 ± 0.12[a,c,d,f-h]
Kidney	28.21 ± 0.31	27.69 ± 0.24[a]	25.80 ± 0.22[a,b]	25.39 ± 0.19[a-c]	27.96 ± 0.28[a,c,d]	27.48 ± 0.34[a,c,d,e]	28.09 ± 0.26[b-d,f]	27.59 ± 0.25[a,c,d,g]	29.22 ± 0.34[a-h]	28.08 ± 0.26[a-d,f-h]	29.47 ± 0.24[a-d,f,g,h,i]	28.43 ± 0.27[b,d,f,h,I,k]
Gut	15.78 ± 0.18	15.52 ± 0.13	14.81 ± 0.21[a,b]	14.51 ± 0.14[a-c]	16.32 ± 0.13[a-d]	15.81 ± 0.17[b-e]	16.48 ± 0.13[a-d,f]	15.95 ± 0.11[c-e,g]	16.14 ± 0.09[a-d,f,]	15.88 ± 0.05[a,b,f-h]	16.11 ± 0.10[a-d,f,h,j]	15.93 ± 0.08[b-e,g,i]
Brain	21.69 ± 0.14	20.88 ± 0.06[a]	18.05 ± 0.28[a,b]	17.84 ± 0.09[a-c]	22.48 ± 0.15[a-d]	22.04 ± 0.18[a-e]	23.02 ± 0.07[a-f]	23.32 ± 0.11[a-g]	20.89 ± 0.14[a,c-e,g,h]	20.15 ± 0.08[a,f,h]	21.16 ± 0.05[a-g,i]	20.73 ± 0.10[f-h,k]
Testes	12.26 ± 0.03	_	10.12 ± 0.02[a]	_	13.08 ± 0.03[a,c]	_	14.13 ± 0.09[a,c,e]	_	14.27 ± 0.05[a,c]	_	13.95 ± 0.04[a,c]	_
Ovary	_	10.08 ± 0.06	_	8.09 ± 0.05[b]	_	10.13 ± 0.04[b,d]	_	10.51 ± 0.04[f]	_	10.29 ± 0.03[b,d,h]	_	10.55 ± 0.10[f,j]

Values represent means ± 1 SD (n = 30 mice per group; that is, 30 male and 30 female mice in each lighting environment per strain)
[a]$P < 0.05$ compared with value for C3H mice in male CWF control group.
[b]$P < 0.05$ compared with value for C3H mice in female CWF control group.
[c]$P < 0.05$ compared with value for C3H mice in male bLAD experimental group.
[d]$P < 0.05$ compared with value for C3H mice in female bLAD experimental group.
[e]$P < 0.05$ compared with value for C57BL/6 mice in male CWF control group.
[f]$P < 0.05$ compared with value for C57BL/6 mice in female CWF control group.
[g]$P < 0.05$ compared with value for C57BL/6 mice in male bLAD experimental group.
[h]$P < 0.05$ compared with value for C57BL/6 mice in female bLAD experimental group.
[i]$P < 0.05$ compared with value for BALB/c mice in male CWF control group.
[j]$P < 0.05$ compared with value for BALB/c mice in female CWF control group.
[k]$P < 0.05$ compared with value for BALB/c mice in male bLAD experimental group.

[3H]thymidine uptake and incorporation that was significantly ($P < 0.001$) greater in bLAD compared with CWF groups in C3H mice for skeletal muscle and lower ($P < 0.001$) for liver tissue and is expressed here as a percentage of total tissue [3H]thymidine uptake and incorporation, at 30.7% ± 0.2% for male mice and 16.0% ± 0.3% for female mice and at 5.0% ± 0.2% for male mice and 4.4% ± 0.1% for female mice, respectively. C57BL/6 and BALB/c mouse strains showed no significant differences between CWF and bLAD in this regard.

We also determined whether skeletal muscle and liver tissue, as metabolically active tissues, displayed circadian rhythms in [3H]thymidine uptake and incorporation over a 24-h day in animals exposed to experimental bLAD compared with control CWF. Male and female mice in all strains exhibited circadian rhythms of [3H]thymidine uptake and incorporation in both skeletal muscle (Figure 10) and liver tissue (Figure 11), with levels under both lighting environments gradually increasing beginning at 0400 and extending into the light phase to a peak at 1600 and then rapidly falling 2 h after onset of dark phase (Table 3). Peak levels of [3H]thymidine uptake and incorporation in skeletal muscle (1600) were significantly ($P < 0.05$) higher in male and female C3H mice in bLAD compared with the same sex in control CWF (Figure 11 A). The integrative means of [3H] thymidine uptake and incorporation in skeletal muscle over a 24-h day were 457.7 dpm/g (bLAD male), 383.6 dpm/g (bLAD female), 300.9 dpm/g (CWF male), and 284.0 dpm/g (CWF female). In contrast, although the circadian rhythm of [3H]thymidine uptake and incorporation in both skeletal muscle (Figure 11 B and C) and liver tissue (Figure 11 A through C) revealed the same acrophase (1600) and nadir (0400), there were no significant differences in the integrative means over the course of a 24-h day. Therefore when combined for sex and lighting environment, the integrative mean of [3H]thymidine uptake and incorporation over the course of a 24-h day for liver and metabolic, and physiologic homeostasis in C3H—but not C57BL/6 or BALB/c—mice.

These trends, as previously reported in humans[29,49,64,65] as well as in albino[23] and nude rats[22] and mice,[24] argue that the C3H mice in bLAD experimental group may not have been aging as rapidly as those in the CWF group. Interestingly, other investigators[74] demonstrated that daily melatonin supplementation to middle-aged rats inhibited body weight gain, reduced epigastric fat, and lowered both plasma leptin and insulin concentrations independent of dietary intake. As suggested in our earlier work, the markedly elevated and extended nocturnal melatonin levels may have been responsible for the more youthful metabolic phenotype of bLAD-exposed C3H mice.

bLAD lighting presents itself as an apparent anomaly in C3H mice, stimulating a nearly 6-fold increase in peak amplitude (approximately 670 pg/mL) of the nocturnal melatonin surge

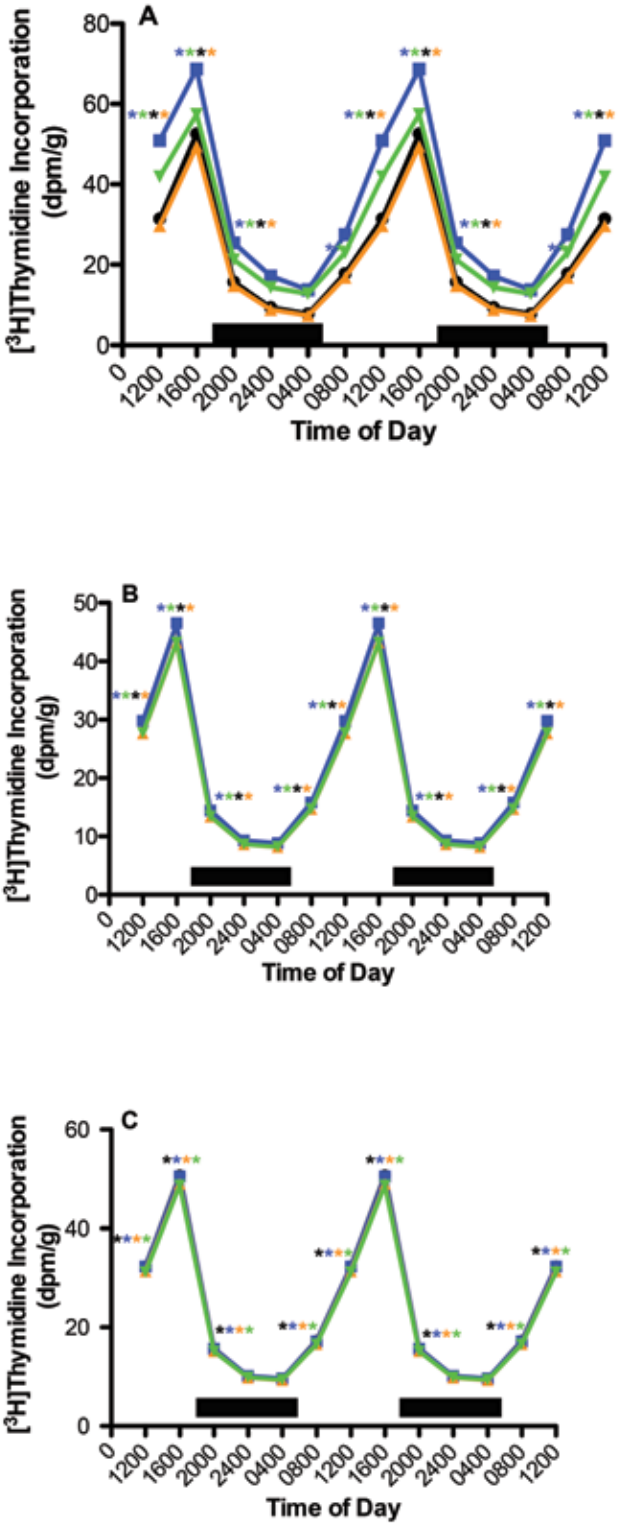

Figure 10. Circadian alterations in [^{3}H]thymidine into skeletal muscle DNA in (A) C3H, (B) C57BL/6, and (C) BALB/c mice male maintained on either CWF control (male, solid black circles; female, solid amber squares) or experimental bLAD (male, solid blue triangles; female, solid green inverted triangles) lighting conditions. Data are plotted twice to better demonstrate rhythmicity. Dark bars represent dark-phase lighting conditions from 1800 to 0600. Concentrations with asterisks are different ($P < 0.05$) from those without asterisks.

tissue in C3H, In the C57BL/6 strain, activated levels of GSK3β, SIRT1, and mTOR were not significantly different between light and dark phases in either skeletal muscle or liver tissues, with the exception of GSK3β in skeletal muscle, whereby phosphoactivation during light phase was 226.6% ± 6.6% higher ($P < 0.05$). In C57BL/6 mice, activated levels in skeletal muscle were higher in male compared with female mice by 40.7% ± 1.2% but markedly lower in liver tissue by 157.4% ± 1.8%. Interestingly, activation of GSK3β, SIRT1, and mTOR in male C57BL/6 mouse skeletal muscle is highest for bLAD compared with CWF lighting, by 43.5% ± 6.7%, at 1200, but this trend was reversed (CWF > bLAD) at 2400, at 45.1% ± 3.3%. Female C57BL/6 mice displayed the opposite effect, with activation of GSK3β, SIRT1, and mTOR being lowest at light phase (1200), with CWF exceeding bLAD by 17.4% ± 1.4%, and highest during the dark phase, with bLAD exceeding CWF by 33.5 ± 2.1%. Activation of GSK3β, SIRT1, and mTOR in male and female C57BL/6 mouse liver followed the trend of bLAD > CWF at 1200 (male, 88.8% ± 4.4%; female, 136.5% ± 10.0%) but reversed at 2400 in both male and female mice, with CWF higher than bLAD (male, 29.7% ± 2.2%; female, 102.4% ± 15.2%).

Discussion

The current findings support the presence of a dynamic, circadian interaction, alignment and balance of animal metabolism and physiology with the light–dark cycle, which may be modulated by exposure to bLAD compared with CWF daytime lighting conditions in the commonly used C3H mouse strain. Light at a given time of day entrains the SCN in an intensity-, duration-, and wavelength-dependent manner, which is essential in the regulation of hormonal circadian rhythms, most notably melatonin, coupled with animal physiology and metabolism.[8,10,47,54,55] In addition, photic history and light exposure during daytime influences nighttime light sensitivity, and attention to daily light exposure patterns has been shown to be important for maintaining health in mammals.[47,49] We previously reported that male, nonpigmented Buffalo rats and pigmented, athymic nude rats and mice maintained under bLAD lighting demonstrated a markedly amplified nocturnal melatonin signal that significantly influenced normal and neoplastic tissue metabolism, signaling activity, and growth, as compared with daytime CWF exposure.[23] Arguably, the significant circadian alterations in melatonin levels in C3H mice exposed to bLAD were most likely responsible for some of the circadian changes in these neurohormones that were observed in the previous and current studies in male and female mice and rats. According to these observations, we tested the hypothesis that bLAD influences circadian patterns of plasma measures of endocrine physiology and metabolism in C3H (melatonin-producing) but not in C57BL/6 and BALB/c (nonmelatonin-producing) inbred mice, 3 commonly used strains in the field of biomedical research. Given the emerging LED lamp technology, with 30% to 40% greater emissions for stimulating melanopsin-containing ipRGC, we compared bLAD with standard CWF lamps commonly used in homes, workplaces, and increasingly in laboratory animal facilities. Our current study demonstrated, for the first time, that long-term exposure to bLAD lighting, compared with CWF lighting, resulted in a markedly augmented amplitude and extended duration of the nocturnal melatonin and that these effects were associated with changes in the circadian dynamics of important plasma indicators of neuroendocrine,

over the 'normal' nocturnal melatonin peak (approximately 121 pg/mL). An earlier study,[45] however, reported elevated nocturnal melatonin levels in male rats exposed to bright, daytime sunlight (enriched in blue-appearing light) over a 13-h period, compared with CWF light, in lab animal rooms over the same period. As demonstrated here and in the earlier studies, the markedly high amplitude and extended duration of the melatonin signal during the dark phase, in effect, prolonged the biologic night for several hours into the light phase. Although intensity and duration may play a role, decreased red- and increased blue-appearing light (Figure 1) could not be ruled out as a causative factor. In addition, we previously suggested that these elevated nighttime melatonin levels in the C3H bLAD group are the result of hyperactivation of alklarylamine-N-acetyl transferase (AANAT), the rate-limiting enzyme in the melatonin synthetic pathway.[43] Inhibition of hepatic melatonin metabolism, nonetheless, cannot be ruled out as a potential contributing factor. In the C3H strain, but not the C57BL/6 and BALB/c strains, we demonstrated that the circadian rhythms of all endocrine physiologic and metabolic analytes in the bLAD group were altered in response to the different characteristics of the blue-enriched LED light, compared with the broad-spectrum CWF light during light phase.

Circadian rhythms for all physiologic and metabolic rhythms in both male and female C3H mice were changed to a lesser or greater degree in response to the altered spectral characteristics of blue-enriched LED light compared with broad-spectrum CWF light during the light phase; these changes did not occur in either the C57BL/6 or BALB/c (melatonin-deplete) mouse strains, arguably the exception that proves the rule. Depending on the factor measured, whether circulating plasma or tissue levels, the variations included changes in rhythm amplitude, phasing, or durations or combinations of these circadian features. These altered rhythms appeared to be completely independent of the SCN-generated rhythms in dietary intake of TFA,[7,8,19-23,51] which were nearly identical for both the control and experimental groups in all mouse strains, indicating that the phasing of overall SCN rhythmicity was intact and not affected by short wavelengths during the light phase. This conclusion was further corroborated by the fact that although the melatonin amplitudes and duration were markedly different in C3H mice, the acrophases of the SCN-driven melatonin rhythms for both CWF and bLAD groups were identical, indicating the lack of a timing effect.

Melatonin exerts regulatory influence on glucose and lactate metabolism, as well as on corticosterone, insulin, and leptin in humans,[58,65] rats[37,42,46,47,66,67] and, clearly, in the C3H mice under study here. The dramatic circadian changes in melatonin level and duration in animals exposed to bLAD could be responsible for some of the circadian changes in these hormones as observed in the present study in C3H mice and our previous studies in rats.[22,23] This argument is further supported by the fact that these hormonal changes were not observed in the other melatonin-nonproducing strains of mice here and in previous bLAD studies.[22-24] Although nighttime melatonin levels in mammals decrease with age,[56] studies in rats[74] have demonstrated that daily melatonin supplementation abrogates these age-related events leading to improved health and wellbeing and extended lifespan.[74] Given that the exact mechanism by which this effect occurs remains unknown, other wavelength-dependent but melatonin-independent factors influencing circadian hormonal and neural outputs from the SCN must also be considered.

Circadian oscillations in arterial plasma glucose and lactate levels, and arterial pO_2 and pCO_2 in all strains were, in general, nearly identical. One exception was the 0800 time point for glucose and lactate that was phase-advanced by 4 h in C3H bLAD group, compared with CWF animals. Nonetheless, the overall 24-h integrated levels were lower under in C3H mice exposed to bLAD lighting, as previously observed in female nude rats,[19] suggesting lower rates of basal metabolism in these animals as compared with the control CWF group. Similarly, circadian variations in the phasing, amplitude, and duration of corticosterone, insulin and leptin, which all have a critical effect on whole-animal metabolism, were also altered in response to exposure to daytime short wavelength-enriched LED light in male and female C3H mice but not in C57BL/6 and BALB/c mice, again corroborating the same changes in these parameters as demonstrated in our previous study in circadian melatonin-producing female nude rats[21] and male Buffalo rats.[23]

Corticosterone, insulin, and leptin levels increase during the aging process in mice for reasons that include decreased activity and increased dietary intake and associated adipose tissue accumulation and body weight gains,[32,66,67,73] in addition to an elevated response to stress.[2,49,54] Increasing corticosterone levels during aging is also associated with the inflammatory response leading to metabolic diseases and cancer,[62,73] as demonstrated in C57BL/6 melatonin-deplete mice. Our results reveal that, although the same corticosterone levels and rhythms over time in both C57BL/6 and BALB/c mice were sustained under CWF or bLAD lighting regimens, they are in fact lower by 23.10% ± 0.32% and 51.63% ± 0.52% in male and female C3H mice (melatonin-producing), respectively, under bLAD compared with CWF light. Insulin levels, required to maintain muscle volume[67] and bone mass,[5] are fundamental physiologic capacities that contribute to functional capacity of the animal and also are associated with the mTOR metabolic pathway,[60] all of which contribute during the aging process to insulin resistance and sensitivity leading to obesity and diabetic disorders.[58,74] Plasma insulin levels, although similar for either male and female C57BL/6 and BALB/c mice in both lighting environments, were lower in male and female C3H mice under bLAD compared with CWF light.

Leptin, critical in the regulation of energy metabolism, also is important for normal skeletal muscle and bone growth[67] Plasma leptin levels, although similar for either male and female C57BL/6 and BALB/c mice in both lighting environments, were lower in male and female C3H mice under bLAD compared with CWF light. Taken together, these findings support the argument that bLAD lighting conditions may help to reduce age-induced inflammatory, obesity, and diabetic responses in the circadian melatonin-replete C3H mice.

In all of the major metabolic tissues that we examined here, TFA concentrations, a known factor that increases during the aging process,[58,62] were significantly higher in the CWF control, compared with the bLAD-exposed experimental C3H mice but not in C57BL/6 and BALB/c, mice. This finding follows a trend of increased dietary intake of the CWF animals over that of the bLAD C3H animals but also parallels the findings relating to final, excised organ weights. Fat tissue, in particular, is an endocrine organ that regulates many autocrine, paracrine, and endocrine factors influencing metabolic function, including adipogenesis, glucose metabolism, the renin-angiotensin system, immune responses, and hemostasis.[62] Fat redistribution to skeletal muscle, liver tissue, and visceral fat tissue as animals age is a marker of dysregulated insulin responsiveness and is associated with increased prevalence of metabolic syndrome.[58,62]

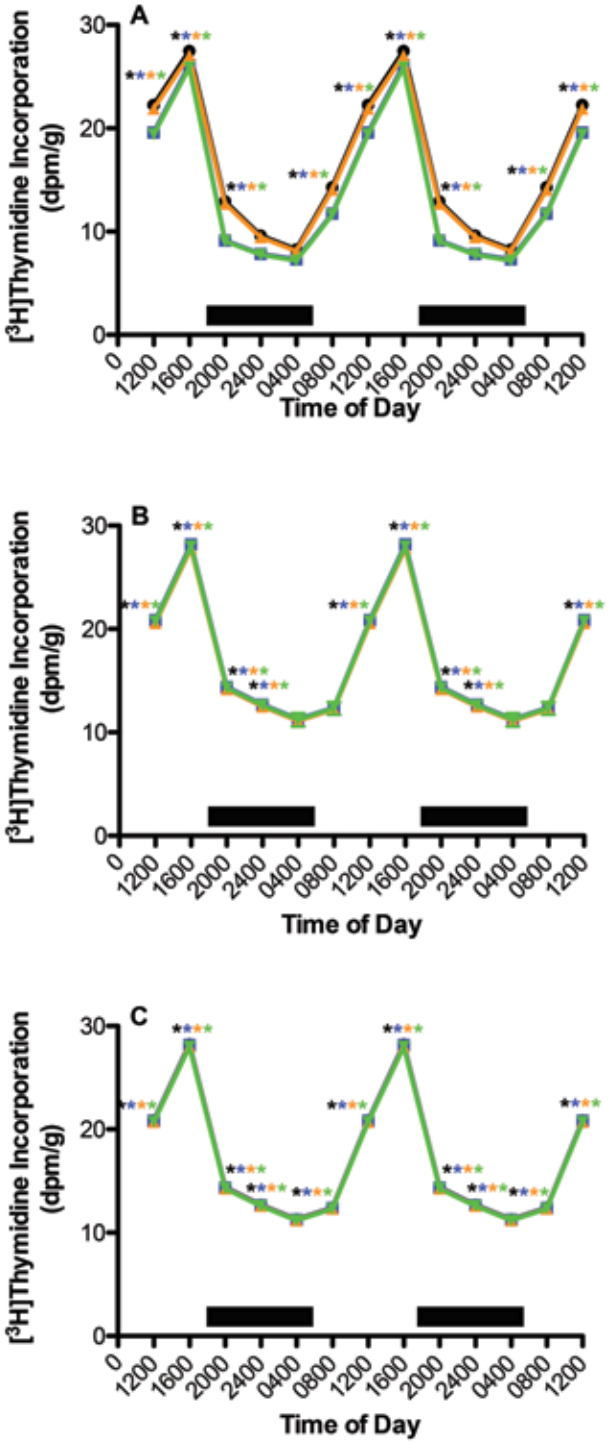

Figure 11. Circadian alterations in [^{3}H]thymidine into liver tissue DNA in (A) C3H, (B) C57BL/6, and (C) BALB/c male maintained on either CWF control (male, solid black circles; female, solid amber squares) or experimental bLAD (male, solid blue triangles; female, solid green inverted triangles) lighting conditions. Data are plotted twice to better demonstrate rhythmicity. Dark bars represent dark-phase lighting conditions from 1800 to 0600. Concentrations with asterisks are different ($P < 0.05$) from those without asterisks.

It is also at the center of processes involved with the determination of lifespan and the onset of age-related diseases. Melatonin inhibits the uptake of TFA in a variety of tissues,[20,21,25] and rats exposed to bLAD compared with CWF lighting at daytime reveal a marked decrease in TFA levels in most tissues including the aforementioned studies. Although TFA concentrations in skeletal muscle, liver, and visceral fat tissues in both C57BL/6 and BALB/c mouse strains were similar under bLAD and CWF lighting conditions, TFA content for male and female C3H mice (cumulative) in these same tissues was lower under bLAD compared with CWF.

In the normal aging process, cellular metabolism in all tissues is crucially dependent upon maintenance of both the mitochondrial and organ proteome.[5,34,45] The overall protein levels of all organs examined, particularly skeletal muscle (corresponding to lean body mass), liver, and adipose tissue, were sustained and even slightly increased in the C3H bLAD group compared with CWF group, as the animals aged.

cAMP, a derivative of ATP and associated with intracellular signal transduction (GS3Kβ, SIRT1, and mTOR),[30,38] plays an important role in lipid homeostasis, energy expenditure, and thermogenesis by increasing lipolysis and fatty acid β-oxidation, and decreases with age. Increases in cAMP levels over time may contribute to its hypolipidemic, antiatherosclerotic effects and have been reported to reverse the effects of aging in cardiomyocytes.[30] The current and previous studies[21-24] strongly suggest a similar effect in C3H circadian melatonin-producing mice maintained under bLAD compared with CWF conditions. Circadian rhythms (Table 3) of cAMP levels in both skeletal muscle and liver in male and female mice of all mouse strains over the course of a 24-h day, but much more so in the C3H strain, are elevated and sustained under bLAD conditions in these 2 critical metabolic tissues, even at 12 wk of age. This situation suggests that enhanced levels of cAMP and its associated kinases function in several biochemical processes, including the regulation of glycogen, glucose, and lipid metabolism, may also be associated with improved function of other important signal transduction and biochemical pathways as the animal ages.

Cumulative values for [^{3}H]thymidine uptake/incorporation into tissue DNA (Table 7) and tissue DNA content (Table 8) revealed unique differences in the major metabolic tissues skeletal muscle and liver) and were most pronounced in the circadian melatonin-producing C3H mouse strain. [^{3}H]Thymidine uptake and incorporation into tissue DNA was elevated markedly in skeletal muscle but was decreased in both liver and adipose tissues under bLAD compared with CWF conditions, whereas DNA content in the respective tissues displayed the opposite effect, possibly suggesting a slower rate of growth over time. Interestingly, a similar observation was made in C3H cardiac tissue, whereas all other tissues in C3H mice maintained under bLAD showed slower rates of growth compared with CWF. This outcome was not the case for the C57BL/6 or BALB/c mouse strains, where there appeared to be minimal-to-no differences in tissues of mice (male compared with male; female compared with females) maintained under either the bLAD or CWF lighting conditions. The circadian rhythms of [^{3}H]thymidine uptake and incorporation into skeletal muscle DNA (Figure 10) or liver DNA (Figure 11) revealed clear differences in C3H mice—but not C57BL/6 and BALB/c mice—maintained under bLAD compared with CWF lighting environments (Table 3).

Several complex factors influence the uptake of thymidine into tissues.[63] The most notable, especially in proliferating and renewing tissues, is the rate of cell turnover; however, small changes in thymidine uptake as seen in the nonrenewal tissues examined in the present investigation do not necessarily reflect a change in the rate of cell proliferation. Uptake and incorporation of bloodborne [^{3}H]thymidine into tissues also depends on the effective size of the complex intracellular and extracellular

Table 8. Effects of cool white fluorescent and blue-enriched LED daytime lighting on tissue DNA levels (mg/g tissue) in C3H, C57BL/6, and BALB/c mice.

	C3H				C57BL/6				BALB/c			
	CWF		bLAD		CWF		bLAD		CWF		bLAD	
Tissue	M	F	M	F	M	F	M	F	M	F	M	F
Liver	2.91 ± 0.03	2.94 ± 0.09	3.02 ± 0.04[a,b]	3.00 ± 0.07[a,b]	2.95 ± 0.10[c,d]	3.03 ± 0.06[a]	2.87 ± 0.13	2.72 ± 0.11[a-g]	2.91 ± 0.12[h]	3.09 ± 0.13[a,b,g-i]	2.80 ± 0.11[c,d,f,j]	3.03 ± 0.08[a,b,e,g-i,k]
Fat	1.13 ± 0.07	1.04 ± 0.02	1.25 ± 0.04[a,b]	1.07 ± 0.03[a-c]	1.28 ± 0.05[a,b]	1.26 ± 0.01[a,b,d]	1.12 ± 0.04[b,c,e,f]	1.14 ± 0.02[c,e,f]	1.16 ± 0.04[c,d]	1.27 ± 0.01[a,b,d,g-i]	1.04 ± 0.02[a,c,e-i,j]	1.11 ± 0.03[b,c,e,f,j]
Muscle	2.74 ± 0.11	2.53 ± 0.09[a]	3.19 ± 0.10[a,b]	2.97 ± 0.08[a-c]	3.07 ± 0.1[a,b,c]	3.03 ± 0.09[a,b]	2.91 ± 0.10[a,b,e]	2.70 ± 0.08[b,c-e,g]	3.11 ± 0.12[a,b,g,h]	2.90 ± 0.06[a-c,h,i]	2.91 ± 0.09[a,b,c,e,i]	2.82 ± 0.07[c-f,i]
Heart	3.01 ± 0.09	2.96 ± 0.04	3.35 ± 0.10[a,b]	3.08 ± 0.05[b,c]	3.02 ± 0.03[b-d]	3.03 ± 0.06	3.00 ± 0.10	3.023 ± 0.06[c]	3.11 ± 0.07[b]	3.10 ± 0.04[b,c]	2.87 ± 0.12[c,d,h,i,j]	3.06 ± 0.08[b,c,k]
Lung	1.99 ± 0.04	1.98 ± 0.03	2.18 ± 0.05[a,b]	2.08 ± 0.04[a-c]	2.23 ± 0.06[a,b,d]	2.18 ± 0.05[a,b,d]	1.97 ± 0.03[c-f]	2.57 ± 0.11[a-c,e-g]	2.22 ± 0.04[a,b,g]	2.22 ± 0.06[a,b,d,g]	2.01 ± 0.05[e,f,h,I,j]	2.12 ± 0.09[b,c]
Kidney	2.76 ± 0.04	2.86 ± 0.03	2.97 ± 0.03[a,b]	2.92 ± 0.04[a-c]	3.10 ± 0.08[a-c,d]	2.90 ± 0.04[a,b,e]	2.92 ± 0.06[a,e]	2.85 ± 0.05[a,c]	3.20 ± 0.04[a,b,d,h]	3.00 ± 0.06[a-d,f,g-h]	3.06 ± 0.04[a-c,d,f-i]	2.93 ± 0.07[a,b,e,i-k]
Gut	3.09 ± 0.04	3.14 ± 0.03	3.35 ± 0.06[a,b]	3.32 ± 0.04[a-c]	3.21 ± 0.03[a-c,d]	3.09 ± 0.08[c,d,e]	3.01 ± 0.11[b-e]	3.02 ± 0.04[b-e]	3.37 ± 0.07[a-h]	3.31 ± 0.05[a,b,f,-h]	2.95 ± 0.08[a,b,d-i,j]	3.09 ± 0.06[c-e,I,j]
Brain	1.35 ± 0.04	1.95 ± 0.06[a]	2.05 ± 0.08[a,b]	2.13 ± 0.06[a-c]	2.14 ± 0.05[a,b]	1.93 ± 0.05[a,c-e]	2.02 ± 0.08[a,d,e,f]	1.83 ± 0.08[a-f]	2.09 ± 0.05[b,f,h]	2.05 ± 0.04[a,f,h]	2.06 ± 0.08[a,b,f,h]	1.90 ± 0.07[a,c-e,i,k]
Testes	2.66 ± 0.03	_	2.85 ± 0.02[a]	_	2.95 ± 0.03[a,c]	_	2.94 ± 0.09[c,d]	_	2.92 ± 0.05[a,c]	_	2.95 ± 0.04[a,c]	_
Ovary	_	2.70 ± 0.06	_	2.78 ± 0.05	_	2.90 ± 0.03[b,d]	_	2.70 ± 0.04[f]	_	2.88 ± 0.03[b,d,h]	_	2.76 ± 0.10[f,j]

Values represent means ± 1 SD (n = 30/group; that is, 30 males and 30 females in each lighting environment per strain).
[a]$P < 0.05$ compared with value for C3H mice in male CWF control group.
[b]$P < 0.05$ compared with value for C3H mice in female CWF control group.
[c]$P < 0.05$ compared with value for C3H mice in male bLAD experimental group.
[d]$P < 0.05$ compared with value for C3H mice in female bLAD experimental group.
[e]$P < 0.05$ compared with value for C57BL/6 mice in male CWF control group.
[f]$P < 0.05$ compared with value for C57BL/6 mice in female CWF control group.
[g]$P < 0.05$ compared with value for C57BL/6 mice in male bLAD experimental group.
[h]$P < 0.05$ compared with value for C57BL/6 mice in female bLAD experimental group.
[i]$P < 0.05$ compared with value for BALB/c mice in male CWF control group.
[j]$P < 0.05$ compared with value for BALB/c mice in female CWF control group.
[k]$P < 0.05$ compared with value for BALB/c mice in male bLAD experimental group.

metabolic pools of DNA precursors and to the proportion of the injected thymidine dose made available to these pools. The availability of injected thymidine is, in turn, dependent upon the vascularity of the target tissues and enzymatic regulation since thymidine is not a normal intermediate in DNA metabolism.[63] Any one or combination of these factors may be potentially under circadian control and influenced by bLAD as suggested by the present data. Clearly, although both skeletal muscle and liver are considered to be nonproliferating tissues, they remain the most metabolically active tissues of the body, and the circadian changes in [^{3}H]thymidine uptake and corresponding modifications by bLAD in C3H mice may have important implications for organ function.

Over the past several years in the field of aging and longevity research, several evolutionarily conserved signaling pathways and regulators for aging have been identified: GSK3β, NAD^+-dependent SIRT1, and mTOR.[30] These key constituents mediate fundamental metabolic and physiologic processes that contribute to cellular and molecular characteristics of aging, such as mitochondrial dysfunction, epigenetic alterations, genomic instability, loss of proteostasis, and several others, and help to determine lifespan in organisms.[12,64] Light and light/dark cycles entrain the SCN (the master biologic clock) through the melatonin signal,[58] and in turn influence circadian oscillation of these important proteins. Under normal circumstances levels of GSK3β, SIRT1, and mTOR decay with aging or disease and significantly affect mitochondrial oxidative phosphorylation in major metabolic tissues such as skeletal muscle and liver. Male mice of the C57BL/6 strain, and much more so of the C3H strain, exhibited higher activation levels of GSK3β, SIRT1, and mTOR in skeletal muscle and liver tissue than female mice during light phase, compared with dark phase, under both CWF and bLAD lighting environments, which correlated well with greater muscle mass and body weight. In addition, phosphorylation of GSK3β, SIRT1, and mTOR in skeletal muscle and liver tissue in both C3H (1200 and 2400) and C57BL/6 (1200) mice (male > female) was highest in animals maintained under bLAD conditions, compared with CWF daytime lighting. Conversely, this effect appeared to be reversed in liver tissue for both strains. In C3H mice activation of the 3 signaling molecules in liver tissue was similar at 1200 and 2400 in CWF, compared with bLAD. In C57BL/6 mice (male and female) activation was higher in liver tissue in bLAD, compared with CWF, at 1200 but reversed at 2400. Nocturnal animals, such as these mice, normally have higher rates of metabolism during the active dark phase than during light phase.[55] The data suggest that amplification of the circadian nighttime melatonin signal in C3H mice (melatonin-producing), compared with C57BL/6 (melatonin-nonproducing) mice, by long-term exposure to bLAD compared with CWF lighting conditions, which extended well into the day time

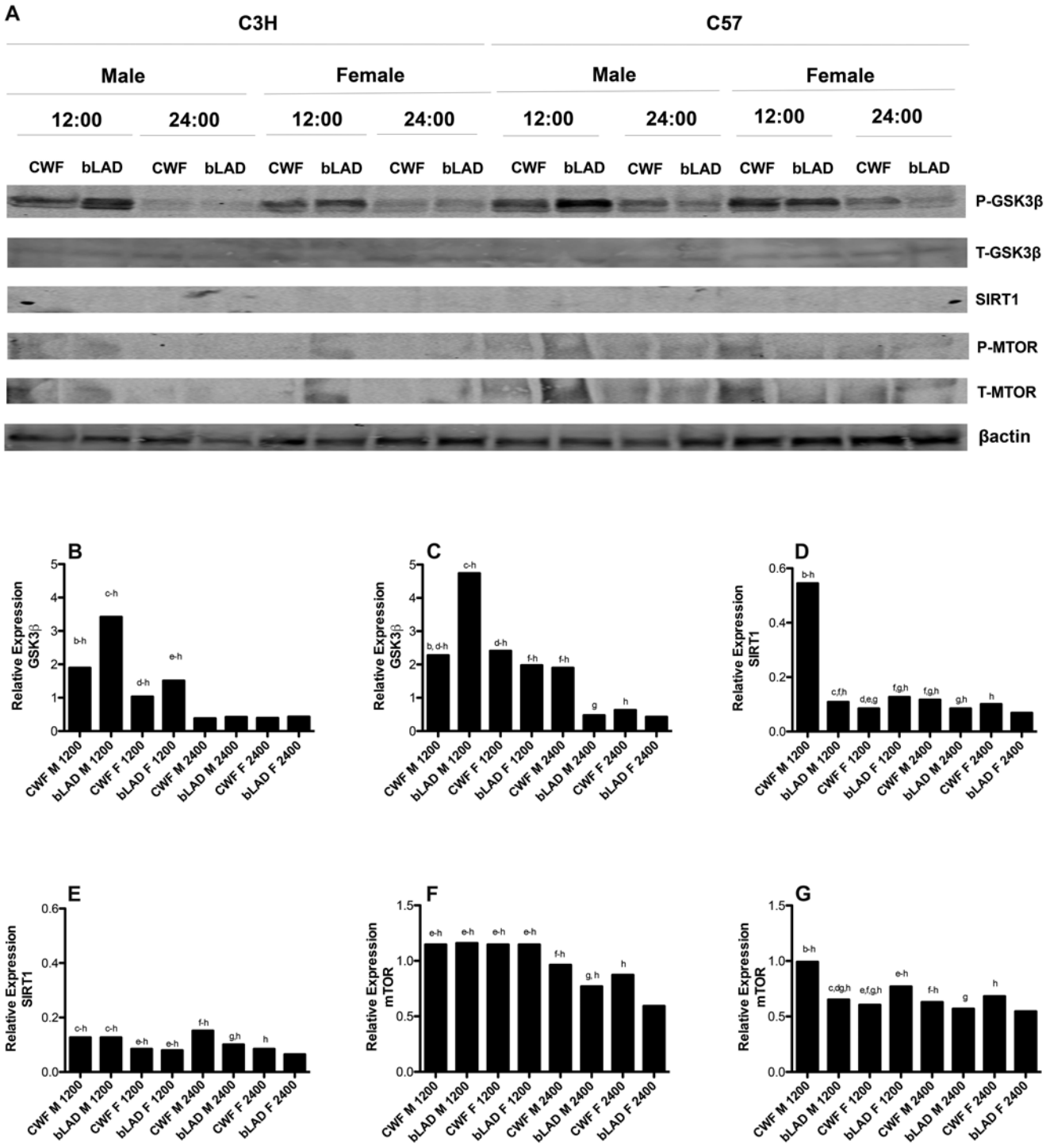

Figure 12. Western blot analysis of the expression of phosphorylated (p) and total (t) forms of GSK3β, SIRT1, and mTOR in (A) skeletal muscle from male and female C3H and C57BL/6 mice exposed to either control CWF or experimental bLAD daytime light at 1200 (CWF, lanes 1, 5, 9, and 13; bLAD, lanes 2, 6, 10, and 14) or 2400 (CWF, lanes 3, 7, 11, and 15; bLAD, lanes 4, 8, 12, and 16); each lane represents results from 5 mouse tissue samples combined. Relative expression (mean ± 1 SD; derived from the densitometric quantitation of the immunoblots) as phosphorylated GSK3β to total protein in C3H (B) C57BL/6 mouse (C) skeletal muscle. Significant ($P < 0.05$) differences from CWF 1200 are indicated as: [a]CWF male (M) 1200, [b]bLAD (M) 1200, [c]CWF female (F) 1200, [d]bLAD F 1200, [e]CWF M 2400, [f]bLAD M 2400, [g]CWF F 2400, and [h]bLAD F 2400. Relative expression (mean ± 1 SD; derived from the densitometric quantitation of the immunoblots) of SIRT1 total protein in (D) C3H and (E) C57BL/6 mouse skeletal muscle. Significant ($P < 0.05$) differences from CWF 1200 are indicated as: [a]CWF male (M) 1200, [b]bLAD (M) 1200, [c]CWF female (F) 1200, [d]bLAD F 1200, [e]CWF (M) 2400, [f]bLAD (M) 2400, [g]CWF (F) 2400, and [h]bLAD (F) 2400. Relative expression (mean ± 1 SD; derived from the densitometric quantitation of the immunoblots) as phosphorylated mTOR to total protein in (F) C3H and (G) C57BL/6 mouse skeletal muscle. Significant ($P < 0.05$) differences from CWF 1200 are indicated as: [a]CWF male (M) 1200, [b]bLAD M 1200, [c]CWF female (F) 1200, [d]bLAD F 1200, [e]CWF (M) 2400, [f]bLAD (M) 2400, [g]CWF (F) 2400, and [h]bLAD (F) 2400.

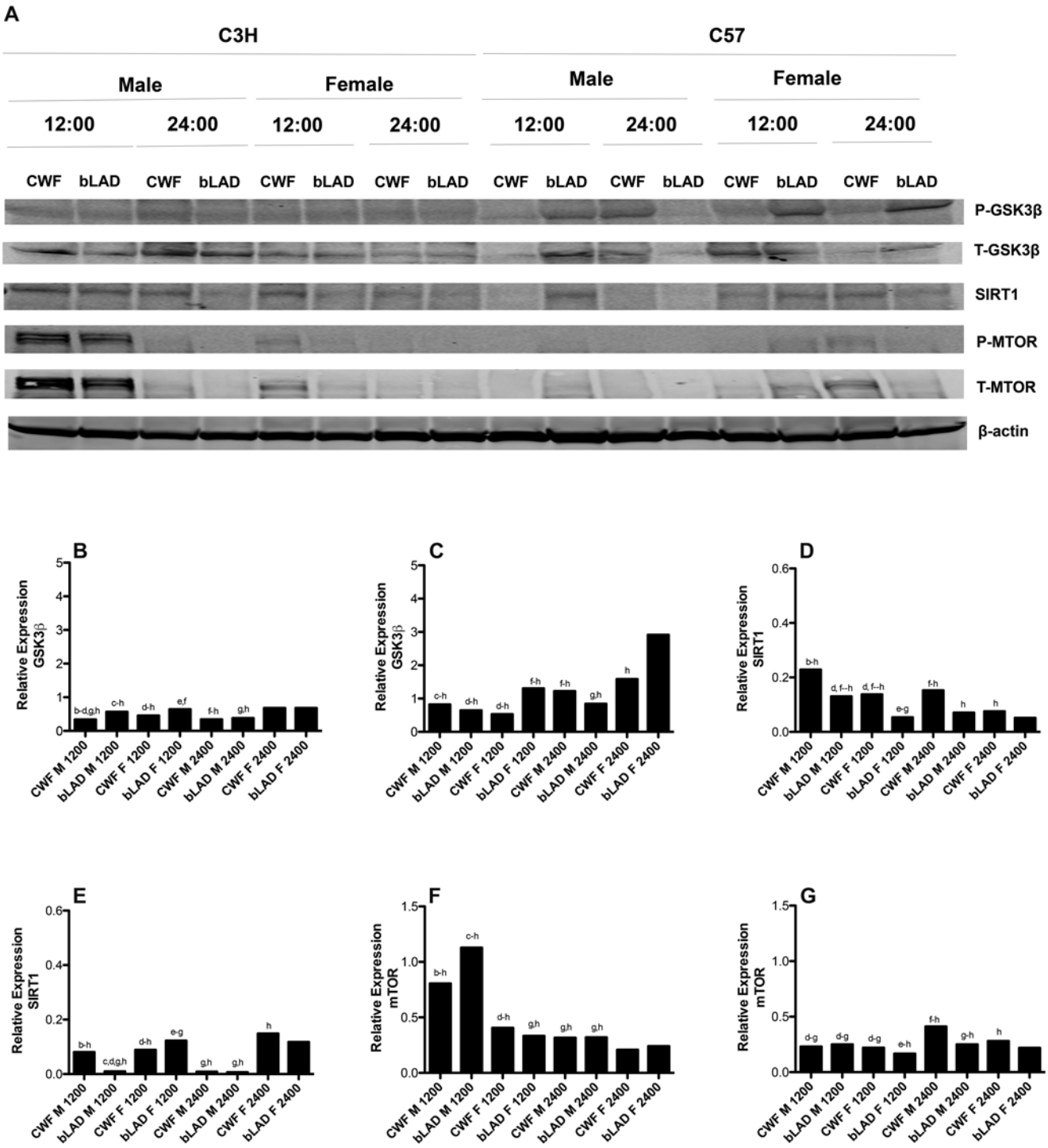

Figure 13. Western blot analysis of the expression of phosphorylated (p) and total (t) forms of GSK3β, SIRT1, and mTOR in (A) liver from male and female C3H and C57BL/6 mice exposed to either control CWF or experimental bLAD daytime light at 1200 (CWF, lanes 1, 5, 9, and 13; bLAD, lanes 2, 6, 10, and 14) or 2400 (CWF, lanes 3, 7, 11, and 15; bLAD, lanes 4, 8, 12, and 16); each lane represents results from 5 mouse tissue samples combined. Relative expression (mean ± 1 SD; derived from the densitometric quantitation of the immunoblots) as phosphorylated GSK3β to total protein in (B) C3H and (C) C57BL/6 mouse liver. Significant ($P < 0.05$) differences from CWF 1200 are indicated as: [a]CWF male (M) 1200, [b]bLAD (M) 1200, [c]CWF female (F) 1200, [d]bLAD F 1200, [e]CWF (M) 2400, [f]bLAD (M) 2400, [g]CWF (F) 2400, and [h]bLAD F 2400. Relative expression (mean ± 1 SD; derived from the densitometric quantitation of the immunoblots) of SIRT1 total protein in (D) C3H and (E) C57BL/6 mouse liver. Significant ($P < 0.05$) differences from CWF 1200 are indicated as: [a]CWF male (M) 1200, [b]bLAD (M) 1200, [c]CWF female (F) 1200, [d]bLAD (F) 1200, [e]CWF (M) 2400, [f]bLAD (M) 2400, [g]CWF (F) 2400, and [h]bLAD (F) 2400. Relative expression (mean ± 1 SD; derived from the densitometric quantitation of the immunoblots) as phosphorylated mTOR to total protein in (F) C3H and (G) C57BL/6 mouse and liver. Significant ($P < 0.05$) differences from CWF 1200 are indicated as: [a]CWF male (M) 1200, [b]bLAD M 1200, [c]CWF female (F) 1200, [d]bLAD (F) 1200, [e]CWF (M) 2400, [f]bLAD (M) 2400, [g]CWF (F) 2400, and [h]bLAD (F) 2400.

hours, may have a unique, albeit positively enhanced, influence on these 2 important metabolic tissues over time as the animal ages. Previous investigations from our laboratory strongly suggest this to be the case.[22-24] The complex interaction between environmental and genetic factors associated with both these unique strains of laboratory mice affects a delicate balance associated with the aging process and animal health and wellbeing.

At this time, a standardized single measurement unit for quantifying light that regulates circadian, neuroendocrine, and neurobehavioral effects is not available. Over the past few years, a consensus position statement was developed among many laboratories worldwide that have examined wavelength regulation of biologic and behavioral effects of light in humans and other species, including rodents, for best practices for measuring and reporting light stimuli.[48,52] A freely available web-based toolbox is now available that permits calculation of effective irradiance experienced by each rodent ipRGC, cone, and rod photoreceptors that are capable of driving circadian, neuroendocrine and neurobehavioral effects.[52] There exist substantial data to support the notion that ipRGC are anatomically and functionally interconnected with the rod and cone systems supporting vision. Physiologic responses to CWF or bLAD light mirror input from all the retinal photoreceptor classes, with the relative importance of each being labile within and between response types. As such the spectral sensitivity of this photoreceptor system is context-dependent.[1,18,29,48,54,55] Using commonly accepted metrics for reporting spectral response functions, such as those in Table 1, is essential for investigators from the standpoint of reproducibility, robustness, and accountability in research. Assuredly, as data using this management system emerges from multiple laboratories, it will become increasingly possible to generate testable hypotheses to predict the spectral characteristics for targeted physiologic responses to light from various light sources, including CWF and bLAD lighting.

Light, in an intensity-, duration-, and wavelength-dependent manner, is essential in regulating mammalian circadian rhythms, and variations in any of these parameters can affect nearly every biologic process associated with animal physiology and metabolism. With regard to the concerns of the laboratory animal science and biomedical research communities, striking a balance between desirable and undesirable effects of light and darkness and lighting technology demands meticulous, informed consideration of context and knowledge of the multitude influences of light on physiology and metabolism. With regard to vision, any wavelength in the visible spectrum may, in principle, activate the system. In contrast, if the objective is to promote ipRGC photoreception in this remarkably sensitive nonvisual system, light sources may be biased toward the blue-appearing region of the visible spectrum during daytime, such as the bLAD light source that we used in this study. For most mammalian species, the nocturnal melatonin signal signifies an essential zeitgeber (timekeeper) responsible for common circadian rhythms of metabolism and physiology that markedly influence animal health and wellbeing and the outcome of scientific investigations. The present study provides compelling evidence that supraphysiologic nocturnal melatonin levels, as evinced in C3H mice exposed to blue-enriched LED light at daytime, may contribute to a heightened circadian organization of the metabolic and hormonal milieu, compared with circadian nonintact (melatonin-nonproducing) C57BL/6 and BALB/c mice—the exception that proves the rule. Further studies in other species, including humans, are warranted to gain an improved understanding regarding the beneficial effects of exposure to daytime blue-enriched LED light and elevated nocturnal melatonin levels in enhancing the homeostatic regulation in laboratory animals fostering improvement of their health and wellbeing.

Acknowledgments

The project described was generously supported by the 2018 Grants for Laboratory Animal Science (GLAS) from the American Association for Laboratory Animal Science (#556216 to RTD), a Tulane University School of Medicine Faculty Pilot Grant (#630540 to DEB and RTD), a National Institutes of Health-National Cancer Institute R56 grant (1 R56 CA193518-01 to SMH and DEB), funds from the Edmond and Lily Safra Chair for Breast Cancer Research and the Tulane Center for Circadian Biology (SMH), and a grant from the Institute for Integrative Health in Baltimore (to GCB and DEB). We acknowledge and are grateful for the technical support of Mr Adam N Danner, Mr Joshua Davis, Ms Joy Ettling, Ms Amy T Pierce, and Mr Cary M. Pfister.

References

1. **Altimus CM, Güler AD, Alam NM, Arman AC, Prusky GT, Sampath AP, Hattar S.** 2010. Rod photoreceptors drive circadian photoentrainment across a wide range of light intensities. Nat Neurosci **13:**1107–1112. https://doi.org/10.1038/nn.2617.
2. **Alves-Simoes M, Coleman G, Canal MM.** 2015. Effects of type of light on mouse circadian behavior and stress levels. Lab Anim **50:**21–29. https://doi.org/10.1177/0023677215588052.
3. **Aschoff J, editor.** 1981. Handbook of behavioral neurobiology, biological rhythms. New York (NY): Plenum Press.
4. **Bachmanov AA, Reed DR, Tordoff MG, Price RA, Beauchamp GK.** 2001. Nutrient preference and diet-induced adiposity in C57BL/6ByJ and 129P3/J mice. Physiol Behav **72:**603–613. https://doi.org/10.1016/S0031-9384(01)00412-7.
5. **Baker BM, Haynes CM.** 2011. Mitochondrial protein quality control during biogenesis and aging. Trends Biochem Sci **36:**254–261. https://doi.org/10.1016/j.tibs.2011.01.004.
6. **Berson DM, Dunn FA, Takao M.** 2002. Phototransduction by retinal ganglion cells that set the circadian clock. Science **295:**1070–1073. https://doi.org/10.1126/science.1067262.
7. **Blask DE, Brainard GC, Dauchy RT, Hanifin JP, Davidson LK, Krause JA, Sauer LA, Rivera-Bermudez MA, Dubocovich ML, Jasser SA, Lynch DT, Rollag MD, Zalatan F.** 2005. Melatonin-depleted blood from premenopausal women exposed to light at night stimulates growth of human breast cancer xenografts in nude rats. Cancer Res **65:**11174–11184. https://doi.org/10.1158/0008-5472.CAN-05-1945.
8. **Blask DE, Dauchy RT, Dauchy EM, Mao L, Hill SM, Greene MW, Belancio VP, Sauer LA, Davidson LK.** 2014. Light exposure at night disrupts host/cancer circadian regulatory dynamics: impact on the Warburg effect, lipid signaling and tumor growth prevention. PLoS One **9:**1–14. https://doi.org/10.1371/journal.pone.0102776.
9. **Brainard GC.** 1989. Illumination of laboratory animal quarters: participation of light irradiance and wavelength in the regulation of the neuroendocrine system. p 69–74. In: Guttman HN, Mench JA, Simmonds RC, editors. Science and animals: addressing contemporary issues, Bethesda (MD): Scientists Center for Animal Welfare.
10. **Brainard GC, Hanifin JP.** 2005. Photons, clocks, and consciousness. J Biol Rhythms **20:**314–325. https://doi.org/10.1177/0748730405278951.
11. **Brainard GC, Hanifin JP.** 2017. Photoreception for human circadian and neurobehavioral regulation. p 829–846. In: Karlickek R, Sun CC, Zissis G, Ma R, editors. Handbook of advanced lighting technology. Berlin: Springer–Verlag.
12. **Chang HC, Guarente L.** 2013. SIRT1 mediates central circadian control in the SCN by a mechanism that decays with aging. Cell **153:**1448–1460. https://doi.org/10.1016/j.cell.2013.05.027.
13. **Collins FS, Tabak LA.** 2014. Policy: NIH plans to enhance reproducibility. Nature **505:**612–613. https://doi.org/10.1038/505612a.
14. **Commission Internationale de l'Eclairage.** 2015. Report on the first international workshop on circadian and neurophysiological photometry 2013, CIE TN 003:2015. Vienna (Austria): CIE.

15. **Commission Internationale de l'Eclairage.** 2018. CIE System for metrology of optical radiation for ipRGC-Influenced Responses to Light. CIE S 026/E:2018. Vienna (Austria): CIE.
16. **Council on Science and Public Health.** [Internet]. 2012. Report 4-A-12. Light pollution: adverse health effects of nighttime lighting. American Medical Association House of Delegates Annual Meeting, Chicago, Illinois. AMA Policy H-135.937 AMA Policy Database. [Cited 9 April 2019]. Available at: http://circadianlight.com/images/pdfs/newscience/American-Medical-Association-2012-Adverse-Health-Effects-of-Light-at-Night.pdf.
17. **Council on Science and Public Health.** [Internet]. 2016. Report 2-A-16. Human and environmental effects of light emitting diode (LED) community lighting. American Medical Association Annual Meeting, Chicago, Illinois, 10–15 June 2016. AMA Policy Resolution 907-I-16. AMA Policy Database. [Cited 9 April 2019]. Available at: https://www.ama-assn.org/sites/ama-assn.org/files/corp/media-browser/public/about-ama/councils/Council%20Reports/council-on-science-public-health/a16-csaph2.pdf.
18. **Dacey DM, Liao HW, Peterson BB, Robinson FR, Smith VC, Pokorny J, Yau KY, Gamlin PD.** 2005. Melanopsin-expressing ganglion cells in primate retina signal color and irradiance and project to the LGN. Nature **433:**749–754. https://doi.org/10.1038/nature03387.
19. **Dauchy RT, Dupepe LM, Ooms TG, Dauchy EM, Hill CR, Mao L, Belancio VP, Slakey LM, Hill SM, Blask DE.** 2011. Eliminating animal facility light-at-night contamination and its effect on circadian regulation of rodent physiology, tumor growth and metabolism: A challenge in the relocation of a cancer research laboratory. J Am Assoc Lab Anim Sci **50:**326–336.
20. **Dauchy RT, Dauchy EM, Hanifin JP, Gauthreaux SL, Mao L, Belancio VP, Ooms TG, Dupepe LM, Jablonski MR, Warfield B, Wren MA, Brainard GC, Hill SM, Blask DE.** 2013. Effects of spectral transmittance through standard laboratory cages on circadian metabolism and physiology in nude rats. J Am Assoc Lab Anim Sci **52:**146–156.
21. **Dauchy RT, Hoffman AE, Wren-Dail MA, Hanifin JP, Warfield B, Brainard GC, Hill SM, Belancio VP, Dauchy EM, Smith K, Blask DE.** 2015. Daytime blue light enhances the nighttime circadian melatonin inhibition of human prostate cancer growth. Comp Med **65:**473–485.
22. **Dauchy RT, Xiang S, Mao L, Brimmer S, Wren MA, Anbalagan M, Hauch A, Frasch T, Rowan BG, Blask DE, Hill SM.** 2014. Circadian and melatonin disruption by exposure to light at night drives intrinsic resistance to tamoxifen therapy in breast cancer. Cancer Res **74:**4099–4110. https://doi.org/10.1158/0008-5472.CAN-13-3156.
23. **Dauchy RT, Wren-Dail MA, Hoffman AE, Hanifin JP, Warfield B, Brainard GC, Xiang S, Yuan L, Hill SM, Belancio VP, Dauchy EM, Smith K, Blask DE.** 2016. Effects of daytime exposure to light from blue-enriched light-emitting diodes on the nighttime melatonin amplitude and circadian regulation of rodent metabolism and physiology. Comp Med **66:**373–383.
24. **Dauchy RT, Wren-Dail MA, Dupepe LM, Dobek GM, Xiang S, Hill SM, Belancio VP, Pierce AT, Blask DE.** 2018. The influence of daytime exposure to blue-enriched LED light on the nighttime melatonin signal and circadian regulation of murine metabolism and physiology. Abstracts presented at the 2018 AALAS National Meeting, Baltimore Maryland, October 28–1 November 2018. J Am Assoc Lab Anim Sci **57:** 607–608.
25. **Diaz B, Blazquez E.** 1986. Effect of pinealectomy on plasma glucose, insulin, and glucagon levels in the rat. Horm Metab Res **18:**225–229. https://doi.org/10.1055/s-2007-1012279.
26. **DiLaura DL, Houser KW, Mistrick RG, Steffy GR, editors.** 2011. Lighting handbook, 10th ed: reference and application. New York (NY): Illuminating Engineering Society of North America.
27. **Ebihara S, Hudson DJ, Marks T, Menaker M.** 1987. Pineal indole melatonin metabolism in the mouse. Brain Res **416:**136–140.
28. **Fonken LK, Aubrecht TG, Melédez-Fernández OH, Weil ZM, Nelson RJ.** 2013. Dim light at night disrupts molecular circadian rhythms and affects metabolism. J Biol Rhythms **28:**262–271. https://doi.org/10.1177/0748730413493862.
29. **Gabel V, Maire M, Reichert SL, Chellappa CF, Schmidt C, Hommes V, Viola AU, Cajochen C.** 2013. Effects of artificial dawn and morning blue light on daytime cognitive performance, well-being, cortisol, and melatonin levels. Chronobiol Int **30:**988–997. https://doi.org/10.3109/07420528.2013.793196.
30. **Gerhart-Hines Z, Dominy JE, Blättler SM, Jedrychowski MP, Banks AS, Lim JH, Chim H, Gygi SP, Puigserver P.** 2011. The cAMP/PKA pathway rapidly activates SIRT1to promote fatty acid oxidation independently of changes in NAD^+. Mol Cell **44:**851–863. https://doi.org/10.1016/j.molcel.2011.12.005.
31. **Hanifin JP, Brainard GC.** 2007. Photoreception for circadian, neuroendocrine, and neurobehavioral regulation. J Physiol Anthropol **26:**87–94. https://doi.org/10.2114/jpa2.26.87.
32. **Harris BN, Saltzman W.** 2013. Effects of aging on hypothalamic-pituitary-adrenal (HPA) axis activity and reactivity in virgin male and female California mice (*Peromyscus californicus*). Gen Comp Endocrinol **186:**41–49. https://doi.org/10.1016/j.ygcen.2013.02.010.
33. **Hattar S, Lucas RJ, Mrosovsky N, Thompson S, Douglas RH, Hankins MW, Lem J, Biel M, Hofman F, Foster RG, Yau KW.** 2003. Melanopsin and rod-cone photoreceptive systems account for all major accessory visual functions in mice photosensitivity. Nature **424:**76–81.
34. **He Q, Heshka S, Labu J, Boxt L, Krasnow N, Marinos E, Gallagher D.** 2009. Smaller organ mass with greater age, except for heart. J Appl Physiol (1985) **106:**1780–1784. https://doi.org/10.1152/japplphysiol.90454.2008.
35. **Heeke DS, White MP, Mele GD, Hanifin JP, Brainard GC, Rollage MD, Winget CM, Holley DC.** 1999. Light-emitting diodes and cool white fluorescent light similarly suppress pineal gland melatonin and maintain retinal function and morphology in the rat. Lab Anim Sci **49:**297–304.
36. **Hughes ME, Hogenesch JB, Kornacker K.** 2010. JKT_CYCLE: and efficient nonparametric algorithm for detecting rhythmic components in genome-scale data sets. J Biol Rhythms **25:**372–380. https://doi.org/10.1177/0748730410379711.
37. **Illnerová H, Vaněcek J, Hoffman K.** 1983. Regulation of the pineal melatonin concentration in the rat (*Rattus norvegicus*) and the Djungarian hamster (*Phodopus sungorus*). Comp Biochem Physiol A Comp Physiol **74:**155–159. https://doi.org/10.1016/0300-9629(83)90727-2.
38. **Imai SI.** 2016. The NAD world 2.0: the importance of the inter-tissue communication mediated by NAMPT/NAD+/SIRT1 in mammalian aging and longevity control. NPJ Syst Biol Appl **2:**1–9. https://doi.org/10.1038/npjsba.2016.18.
39. **Institute for Laboratory Animal Research.** 2011. Guide for the care and use of laboratory animals, 8th ed. Washington (DC): National Academies Press.
40. **Illuminating Engineering Society of North America.** 2008. Light and human health: An overview of the impact of optical radiation on visual, circadian, neuroendocrine, and neurobehavioral responses, IED TM-18-08. New York (NY): Illuminating Engineering Society of North America.
41. **Illuminating Engineering Society of North America.** [Internet]. 2017. IES board position on AMA CSAPH Report 2-A-16, human and environmental effects of light emitting diode (LED) community lighting. [Cited 9 June 2019]. Available at: https://www.ies.org/about-outreach/position-statements/ies-board-position-on-ama-csaph-report-2-a-16-human-and-environmental-effects-of-light-emitting-diode-led-community-lighting/
42. **Kalsbeek A, Strubbe JH.** 1998. Circadian control of insulin secretion is independent of the temporal distribution of feeding. Physiol Behav **63:**553–558. https://doi.org/10.1016/S0031-9384(97)00493-9.
43. **Kennaway DJ, Voultsios A, Varcoe TJ, Moyer RW.** 2002. Melatonin in mice: rhythms, response to light, adrenergic stimulation, and metabolism. Am J Physiol Regul Integr Comp Physiol **282:**R358–R365. https://doi.org/10.1152/ajpregu.00360.2001.
44. **Klein DC, Weller JL.** 1972. Rapid light-induced decrease in pineal serotonin N-acetyltransferase activity. Science **177:**532–533. https://doi.org/10.1126/science.177.4048.532.
45. **Laakso ML, Porkka-Heiskane T, Alila A, Peder M, Johansson G.** 1988. Twenty-four-hour patterns of pineal melatonin and pituitary

and plasma prolactin in male rats under 'natural' and artificial lighting conditions. Neuroendocrinology **48:**308–313. https://doi.org/10.1159/000125027.

46. **Lettieri-Barbato D, Cannata SM, Casagrande V, Ciriolo MR, Aquilano K.** 2018. Time-controlled fasting prevents aging-like mitochondrial changes induced by persistent dietary fat overload in skeletal muscle. PLoS One **13:**1–16. https://doi.org/10.1371/journal.pone.0195912.
47. **Lima FB, Machado UF, Bartol I, Seraphim PM, Sumida DH, Moraes SMF, Hell NS, Okamotot NM, Saad MJ, Carvalho CR, Cipolla-Neto J.** 1998. Pinealectomy causes glucose intolerance and decreases adipose cell responsiveness to insulin in rats. Am J Physiol **275:**E934–E941.
48. **Lucas RJ, Pierson SN, Berson DM, Brown TM, Cooper HM, Czeisler CA, Figueiro MG, Gamlin PD, Lockely SW, O'Hagan JB, Price LLA, Provencio I, Skenen DJ, Brainard GC.** 2014. Measuring and using light in the melanopsin age. Trends Neurosci **37:**1–9. https://doi.org/10.1016/j.tins.2013.10.004.
49. **Lunn RM, Blask DE, Coogan AN, Figueiro MG, Gorman MR, Hall JE, Hansen J, Nelson RJ, Panda S, Smolensky MH, Stevens RG, Turek FW, Vermeulen R, Carreòn T, Caruso CC, Lawson CC, Thayer KA, Twery MJ, Ewens AD, Garner SC, Schwingl PJ, Boyd WA.** 2017. Health consequences of electric lighting practices in the modern world: A report on the National Toxicology Program's workshop on shift work at night, artificial light at night, and circadian disruption. Sci Total Environ **607-608:**1073–1084. https://doi.org/10.1016/j.scitotenv.2017.07.056.
50. **Moore RY, Lenn NJ.** 1972. A retinohypothalamic projection in the rat. J Comp Neurol **146:**1–14.https://doi.org/10.1002/cne.901460102.
51. **Nelson DL, Cox NM.** 2005. Hormonal regulation of food metabolism, p 881–992. In: Lehninger AL, Nelson DL, Cox MM, editors. Lehninger principles of biochemistry. New York (NY): WH Freeman.
52. **Neufield Department of Clinical Neurosciences Medical Sciences Division.** [Internet]. 2016. Rodent Toolbox v1.xlsx. [Cited 24 February 2016]. Available at: http://ww.eye.ox.ac.uk/team/principal-investigators/stuart-pierson
53. **Panda S, Provencio I, Tu DC, Pires SS, Rollag MD, Castrucci AM, Sato TK, Wiltshire T, Andahazy M, Kay SA, Van Gelder RN, Hogenesch JB.** 2003. Melanopsin is required for non-image-forming photic responses in blind mice. Science **301:**525–527. https://doi.org/10.1126/science.1086179.
54. **Pattison PM, Tsao JY, Brainard GC, Bugbee B.** 2018. LEDs for photons, physiology and food. Nature **563:**493–500. https://doi.org/10.1038/s41586-018-0706-x.
55. **Peirson SN, Brown LA, Pothecary CA, Benson LA, Fisk AS.** 2018. Light and the laboratory mouse. J Neurosci Methods **300:**26–36. https://doi.org/10.1016/j.jneumeth.2017.04.007.
56. **Reiter RJ.** 1991. Pineal gland: interface between photoperiodic environment and the endocrine system. Trends Endocrinol Metab **2:**13–19. https://doi.org/10.1016/1043-2760(91)90055-R.
57. **Reiter RJ, Tan DX, Korkanz A, Erren TC, Piekarski C, Tamura H, Manchester LC.** 2007. Light at night, chronodisruption, melatonin suppression, and cancer risk: a review. Crit Rev Oncog **13:**303–328. https://doi.org/10.1615/CritRevOncog.v13.i4.30.
58. **Reiter RJ, Tan DX, Korkmaz A, Ma S.** 2012. Obesity and metabolic syndrome: association with chronodisruption, sleep deprivation, and melatonin suppression. Ann Med **44:**564–577. https://doi.org/10.3109/07853890.2011.586365.
59. **Roseboom PH, Namboordiri MA, Zimonjic DB, Popescu NC, Rodriguez IR, Gastel JA, Klein DC.** 1998. Natural melatonin "knockdown" in C57BL/6J mice: rare mechanism truncates serotonin *N*-acetyltransferase. Brain Res Mol Brain Res **63:**189–197. https://doi.org/10.1016/S0169-328X(98)00273-3.
60. **Sato S, Solanas G, Peixoto FO, Bee L, Symeonidi A, Schmidt MS, Brenner C, Masri S, Benitah SA, Sassone-Corsi P.** 2017. Circadian reprogramming in the liver identifies metabolic pathways of aging. Cell **170:**664–677e11. https://doi.org/10.1016/j.cell.2017.07.042.
61. **Scholtens RM, van Munster BC, van Kempen MF, de Rooij SE.** 2016. Physiological melatonin levels in healthy older people: a systemic review. J Psychosom Res **86:**20–27. https://doi.org/10.1016/j.jpsychores.2016.05.005.
62. **Sepe A, Tchkonia T, Thomou T, Zamboni M, Kirkland JL.** 2011. Aging and regional differences in fat cell progenitors—a mini review. Gerontology **57:**66–75. https://doi.org/10.1159/000279755.
63. **Steel GG, Lamerton LF.** 1964. The turnover of tritium from thymidine in tissues of the rat. Exp Cell Res **37:**117–131. https://doi.org/10.1016/0014-4827(65)90162-X.
64. **Sletten TL, Revell VL, Middleton B, Lederle KA, Skene DJ.** 2009. Age-related changes in acute and phase-advancing responses to monochromatic light. J Biol Rhythms **24:**73–84. https://doi.org/10.1177/0748730408328973.
65. **Tähkämö L, Partonen T, Pesonen AK.** 2018. Systematic review of light exposure impact on human circadian rhythm. Chronobiol Int **36:**151–170. https://doi.org/10.1080/07420528.2018.1527773.
66. **Templeman NM, Flibotte S, Chik JHL, Sinha S, Lim GE, Foster LJ, Nislow C, Johnson JD.** 2017. Reduced circulating insulin enhances insulin sensitivity in old mice and extends lifespan. Cell Reports **20:**451–463. https://doi.org/10.1016/j.celrep.2017.06.048.
67. **Turner RT, Philbrick KA, Kuah A, Branscu AJ, Iwaniec UT.** 2017. Role of oestrogen receptor signaling in skeletal response to leptin in female *ob/ob* mice. J Endocrinol **233:**357–367. https://doi.org/10.1530/JOE-17-0103.
68. **US Department of Energy.** [Internet]. 2016. MS-SSLC 2016 The Light Post -Official MSSLC e-Newsletter. June [Cited 09 June 2019]. Available at: https://www.energy.gov/sites/prod/files/2016/06/f32/postings_06-21-16.pdf.
69. **Vivien-Roels B, Malan A, Rettori MC, Delagrange P, Jeanniot JP, Pevet P.** 1998. Daily variations in pineal melatonin in inbred and outbred mice. J Biol Rhythms **13:**403–409. https://doi.org/10.1177/074873098129000228.
70. **Vollrath L, Huesgen A, Manz B, Pollow K.** 1988. Day/night serotonin levels in the pineal gland of male BALB/c mice with melatonin deficiency. Acta Endocrinol (Copenh) **117:**93–98. https://doi.org/10.1530/acta.0.1170093.
71. **von Gall C, Lewy A, Schomerus C, Vivien-Roels B, Pevet P, Korf HW, Stehle JH.** 2000. Transcription factor dynamics and neuroendocrine signaling in the mouse pineal gland: a comparative analysis of melatonin-deficient C57BL mice and melatonin-proficient C3H mice. Eur J Neurosci **12:**964–972. https://doi.org/10.1046/j.1460-9568.2000.00990.x.
72. **Weng S, Estevez ME, Berson DM.** 2013. Mouse ganglion-cell photoreceptors are driven by the most sensitive rod pathway and by both types of cones. PLoS One **8:**1–13. https://doi.org/10.1371/journal.pone.0066480.
73. **Wolden-Hanson T.** 2010. Body composition and aging, p 64–83. In: Mobbs CV, Hof PR, editors. Interdisciplinary topics in gerontology, vol 37. New York (NY): Karger.
74. **Wolden-Hanson T, Mitton DR, McCants RL, Yellon SM, Wilkinson CW, Matsumoto AM, Rasmussen DD.** 2000. Daily melatonin administration to middle-aged rats suppresses body weight, intraabdominal adiposity, plasma leptin and insulin independent of food intake and total body fat. Endocrinology **141:**487–497. https://doi.org/10.1210/endo.141.2.7311.